Dedektör Teknolojilerinde Yeni Trendler

Burak Bilki

İstanbul Beykent Üniversitesi
Türk Hızlandırıcı ve Işınım Laboratuvarı
burak.bilki@cern.ch

Ölçülebilir Parçacıklar

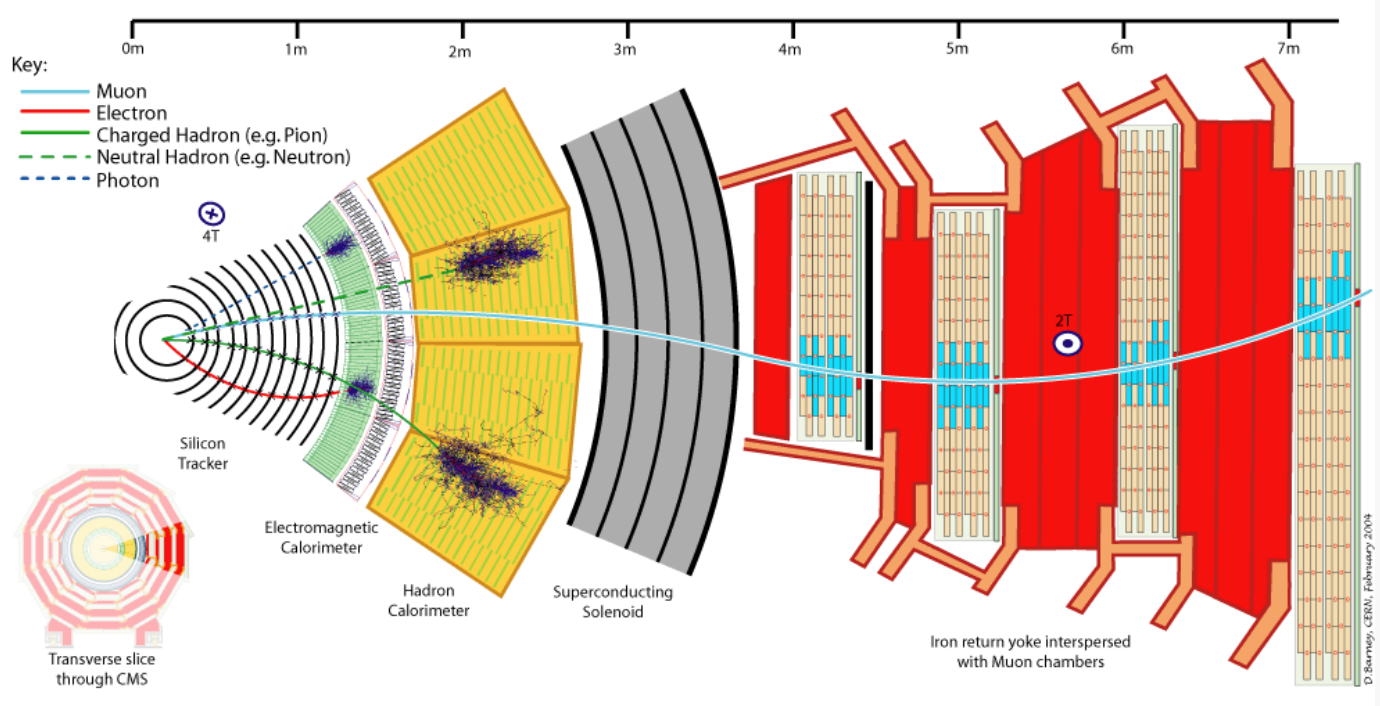

https://cms.cern/book/export/html/1618

particle		constituents	Mass [MeV]	Lifetime τ [s]	$c\tau$
Electron/Positron	$e^{\pm}$		0.511	∞	∞
(Anti)Muon	$\mu^{\pm}$		105.7	2.2×10^{-6}	659 m
(Anti)Tauon	$\tau^{\pm}$		1777	2.9×10^{-13}	87 μm
Electron-Neutrino	ν_e		$< 3 \times 10^{-6}$ *	∞	∞
Muon-Neutrino	ν_μ		<0.19 *	∞	∞
Tau-Neutrino	ν_τ		<18.2 *	∞	∞
Photon	γ		0	∞	∞
Charged Pions	$\pi^{\pm}$	$u\bar{d}$, $d\bar{u}$	140	2.6×10^{-8}	7.8 m
Charged kaons	$K^{\pm}$	$u\bar{s}$, $s\bar{u}$	494	1.2×10^{-8}	3.7 m
Neutral kaons	K^0_L, K^0_S	$d\bar{s}$, $s\bar{d}$	497	5.1×10^{-8}, 8.9×10^{-11}	15.5 m, 2.7 cm
D-Mesons	$D^{\pm}$	$c\bar{d}$, $d\bar{c}$	1869	1.0×10^{-12}	315 μm
	D^0	$c\bar{u}$, $u\bar{c}$	1864	4.1×10^{-13}	123 μm
	$D^{\pm}_s$	$c\bar{s}$, $s\bar{c}$	1969	4.9×10^{-13}	147 μm
B-Mesons	$B^{\pm}$	$u\bar{b}$, $b\bar{u}$	5279	1.7×10^{-12}	502 μm
	B^0	$b\bar{d}$, $d\bar{b}$	5279	1.5×10^{-12}	462 μm
	B^0_s	$s\bar{b}$, $b\bar{s}$	5370	1.5×10^{-12}	438 μm
	$B^{\pm}_c$	$c\bar{b}$, $b\bar{c}$	~6400	$\sim 5.0 \times 10^{-13}$	~150 μm
Proton	p	uud	938.3	$>10^{25}$ y	∞
Neutron	n	udd	939.6	885.7 s	10^8 km
Lambda	Λ	uds	1116	2.6×10^{-10}	7.9 cm
	Λ^+_c	udc	2285	2.0×10^{-13}	60 μm
	Λ_b	udb	5624	1.2×10^{-12}	368 μm
Sigma	Σ^+	uus	1189	8.0×10^{-11}	2.4 cm
	Σ^-	dds	1198	1.5×10^{-10}	4.4 cm
Xi	Ξ^0	uss	1315	2.9×10^{-10}	8.7 cm
	Ξ^-	dss	1321	1.6×10^{-10}	4.9 cm
	Ξ^+_c	usc	2466	4.4×10^{-13}	132 μm
	Ξ^0_c	dsc	2472	$\sim 1.0 \times 10^{-13}$	~29 μm
Omega	Ω^-	sss	1673	8.2×10^{-11}	2.5 cm
	Ω^0_c	ssc	2698	6.0×10^{-14}	19 μm

Dedektör yalnızca “kararlı” parçacıkları görebilir:

Elektron, müon, pion, kaon, foton, proton, nötron

https://repository.cern/records/7e0p4-dy664

Dedektörlerin Tarihsel Gelişimi

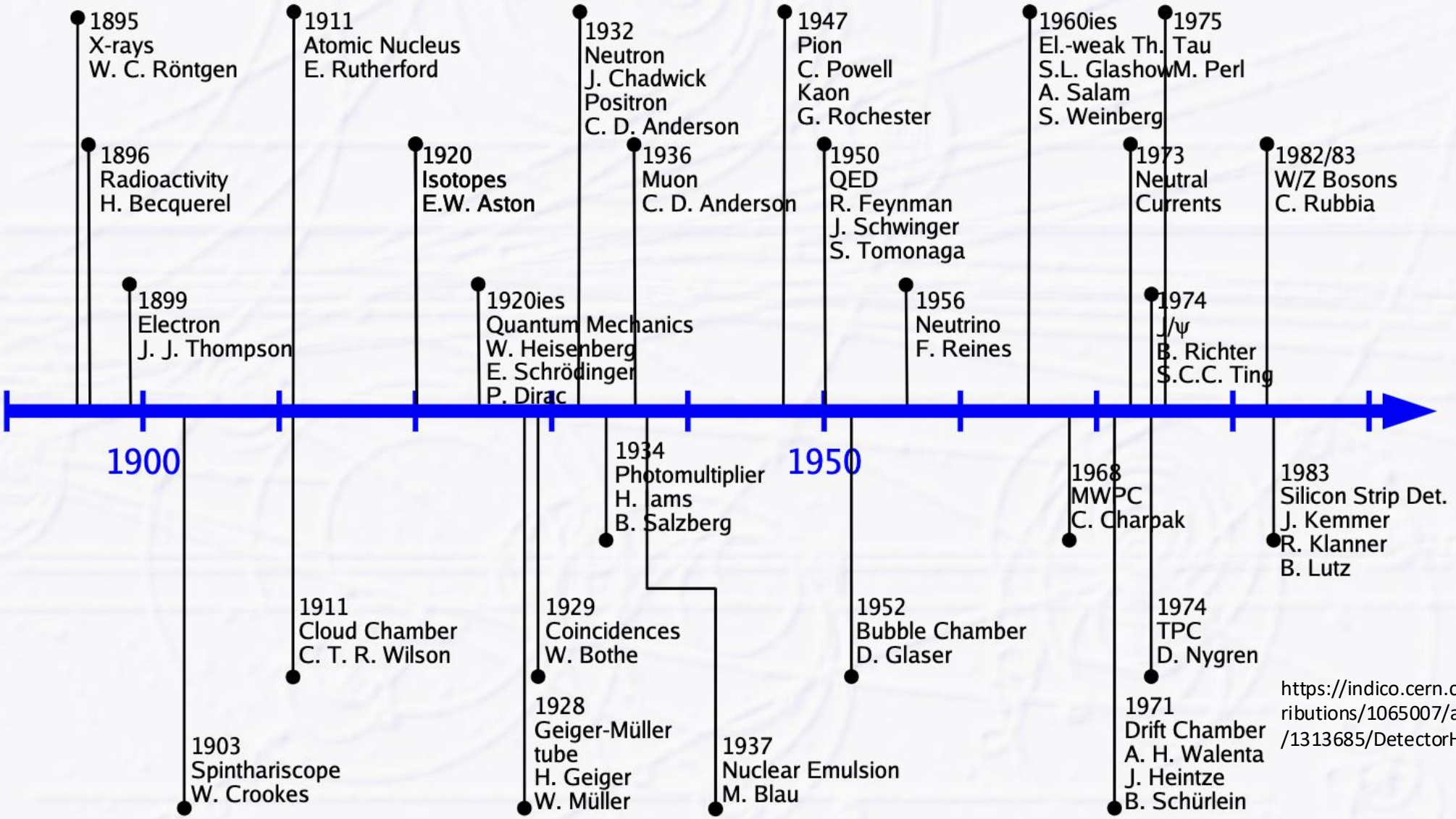

https://indico.cern.ch/event/43007/contributions/1065007/attachments/927852/1313685/DetectorHistory.pdf

Parçacıkların Tespiti ve Ölçümü

- Detection = particle counting (is there a particle?)
- Identification = measurement of mass and charge of the particle
  (most elementary particle have Ze=±1)

How:

- charged particles are deflected by B fields such that:

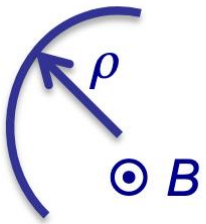

$$\rho = \frac{p}{ZeB} \propto \frac{p}{Z} = \frac{\gamma \boxed{m_0 \beta c}}{Z}$$

p = particle momentum
m_0 = rest mass
βc = particle velocity

- particle velocity measured with time-of-flight method

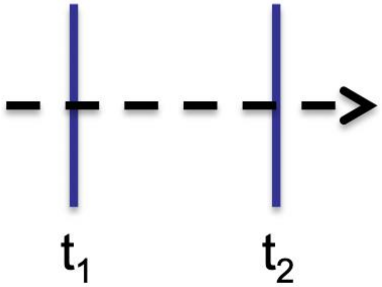

$$\beta \propto \frac{1}{\Delta t}$$

Parçacıkların Tespiti ve Ölçümü

- Detection = particle counting (is there a particle?)
- Identification = measurement of mass and charge of the particle
  (most elementary particle have Ze=±1)

How:

- kinetic energy determined via a calorimetric measurement

$$E^{kin} = (\gamma - 1) m_0 c^2 \qquad \gamma = \frac{1}{\sqrt{1+\beta^2}}$$

- for Z=1 the mass is extracted from E^{kin} and p
- to determine Z (particle charge) a Z-sensitive variable is e.g. the ionization energy loss

$$\frac{dE}{dx} \propto \frac{Z^2}{\beta^2} \ln\left(a\beta^2\gamma^2\right)$$

a = material-dependent constant

Parçacık - Madde Etkileşimleri

Yüklü ve nötr parçacıklar için etkileşimler farklıdır.

Elektromanyetik ve güçlü etkileşimler için süreçlerin "ölçeği" farklıdır.

- Yüklü parçacıkların (e, μ, π, K, p) tespiti (İyonizasyon, Bremsstrahlung, Çerenkov …)
- γ-ışınlarının tespiti (Foto/Compton etkisi, çift üretimi)
- Nötronların tespiti (güçlü etkileşim)
- Nötrinoların tespiti (zayıf etkileşim)

Ölçüm Teknikleri

Parçacık	Etkileşim	Ölçüm Yöntemi	Ölçüm Cihazları
Elektron/MIP	İyonizasyon	Yük	**Silikon, gazlı dedektörler + yük ölçüm sistemi**
Elektron/Hadron/ MIP	İyonizasyon/Uyarım	Optik	**Sintilatörler + fotodedektörler + yük ölçüm sistemi**
Elektron/Hadron/ MIP	Foton yayılımı	Optik	**Radyatörler (Cerenkov/geçiş) + fotodedektörler + yük ölçüm sistemi**
Elektron/Pozitron/ Foton	Bremsstrahlung, çift oluşumu	Yük, optik	**Elektromanyetik Kalorimetre**
Hadron (nötron)	Elastik ve nükleer etkileşimler	Yük, optik	**Hadron Kalorimetresi**
Nötrino	Zayıf etkileşim	Yük, optik	**Geniş hacimli asal sıvı dedektörleri**

Güncel Büyük Çaplı Deneyler

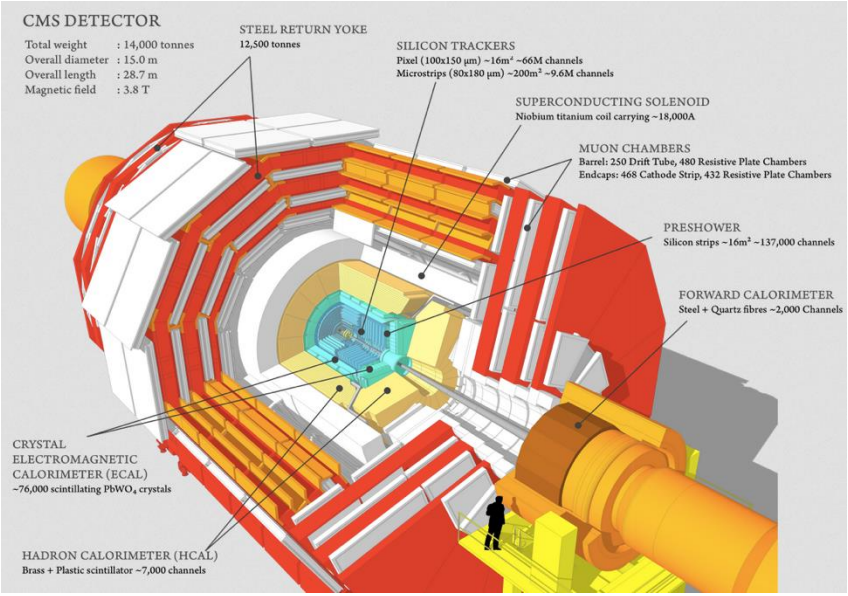

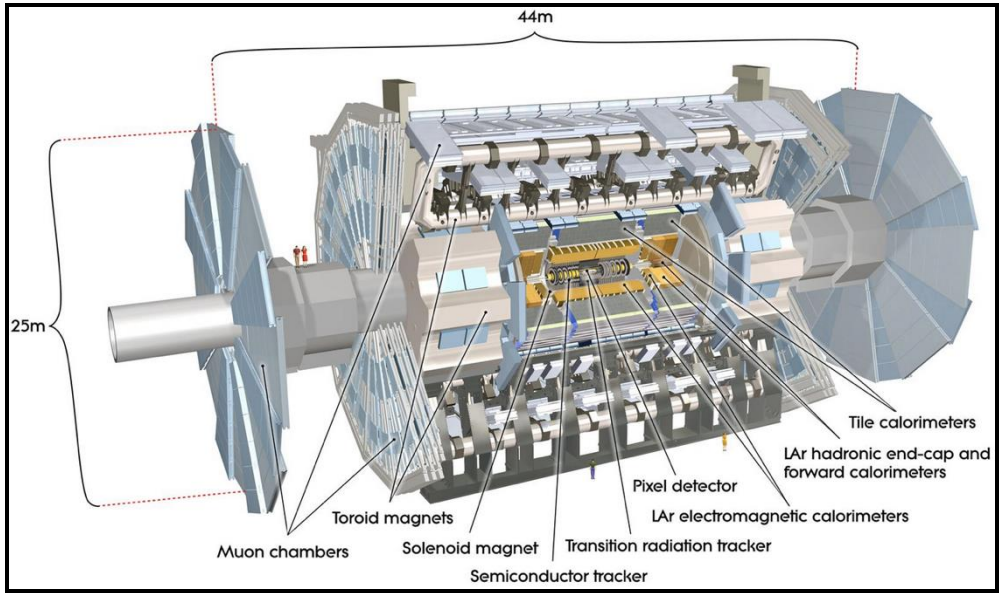

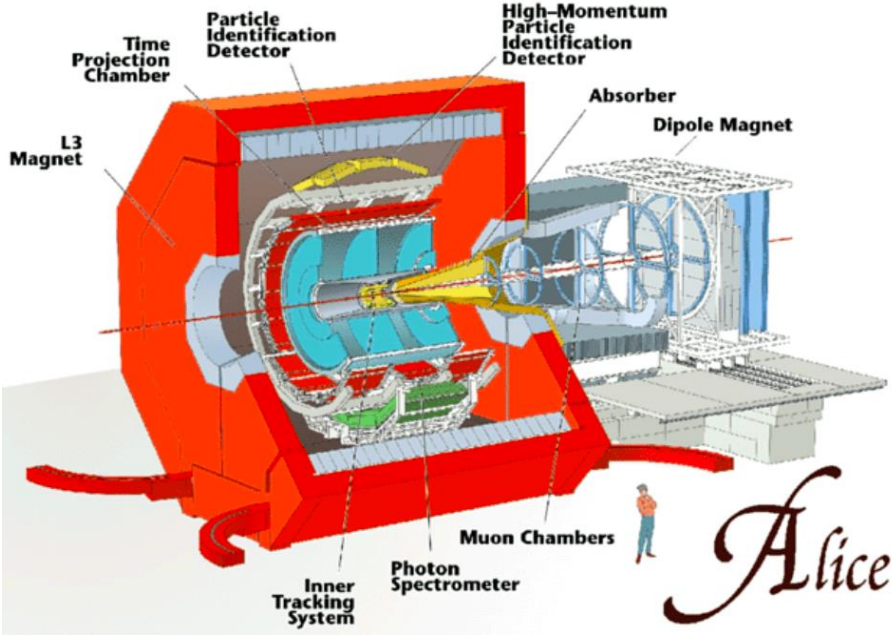

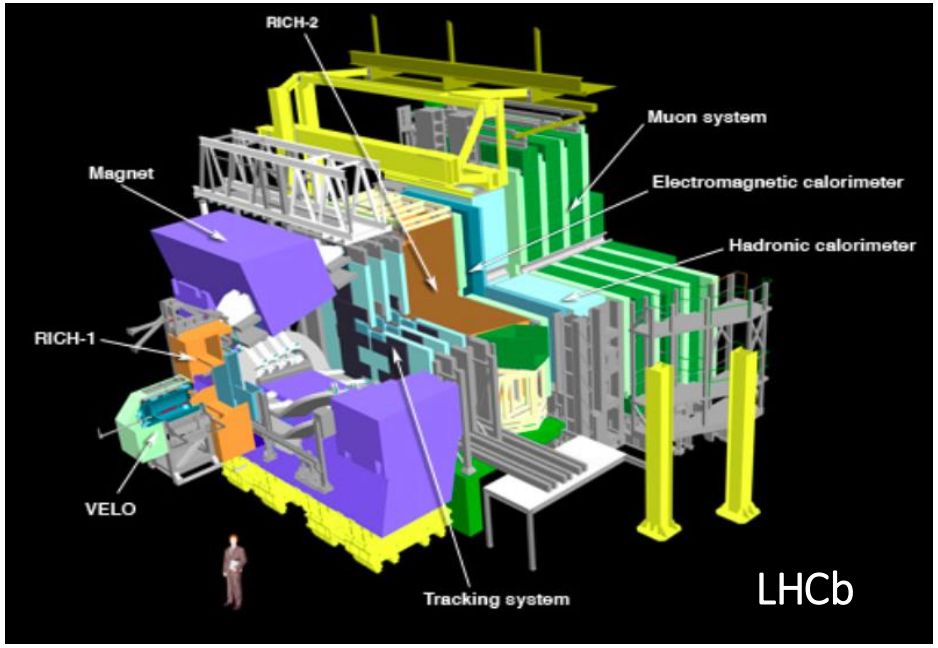

Gelecek Büyük Çaplı Deneyler - I

CLIC

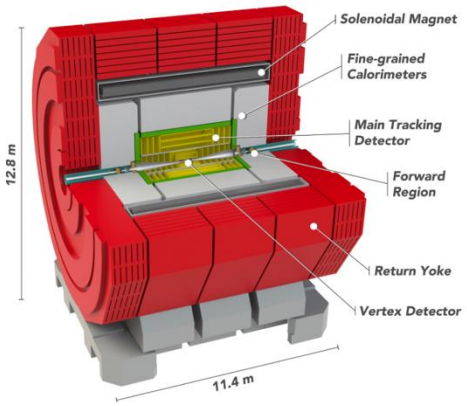

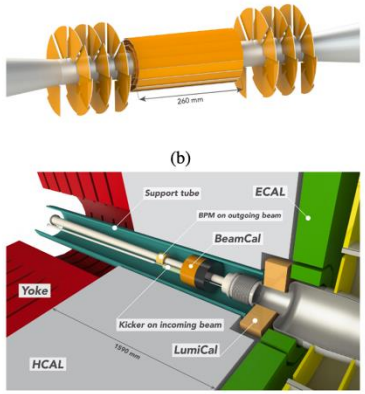

https://arxiv.org/pdf/1812.07987.pdf

FCC-hh Reference Detector

- 4T, 10m solenoid, unshielded
- Forward solenoids, unshielded
- Silicon tracker
- Barrel ECAL LAr
- Barrel HCAL Fe/Sci
- Endcap HCAL/ECAL LAr
- Forward HCAL/ECAL LAr

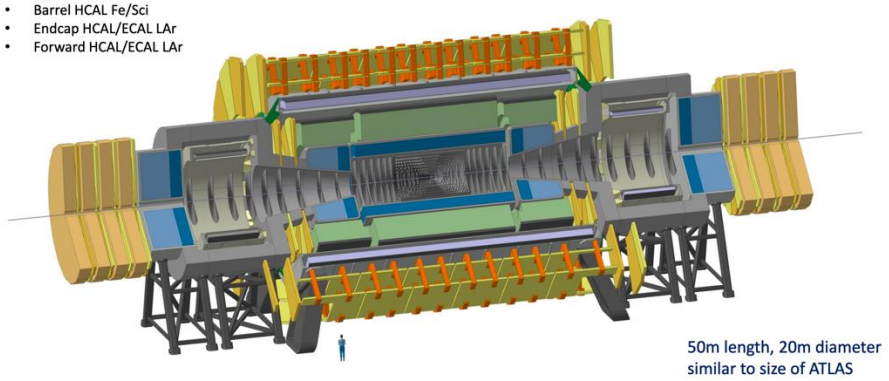

https://indico.cern.ch/event/727555/contributions/3461232/attachments/1869213/3075082/fcc_hh_detector_brussels_june_2019_riegler.pdf

FCC-he Detector Study

Peter Kostka et al.

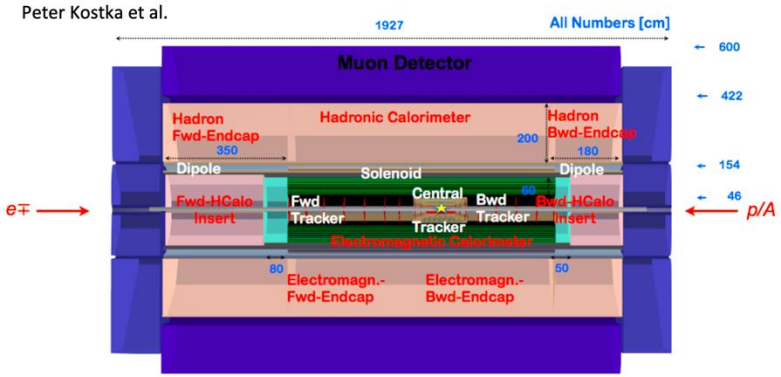

- Very preliminary FCC detector design: extension of LHeC baseline detector
- Dimensions 20 x 12 m, transverse and longitudinal (fwd) sizes scaled w.r.t. LHeC
- Assumption of similar electron beam steering dipoles as in LHeC baseline design

Note added: LHeC→HE-LHC→FCC-he: 1→1.4→2 scaling the fwd dimension

Alessandro Polini 14.4.

https://indico.cern.ch/event/438866/contributions/1085066/attachments/1258651/1859171/ehsumRome.pdf

FCC-ee detector design concepts

- Two designs studied so far

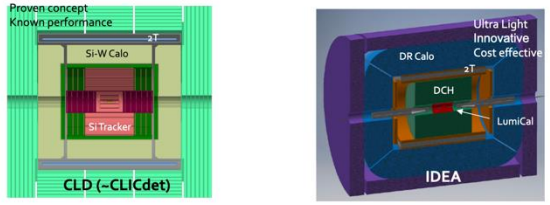

- It was demonstrated that detectors satisfying the requirements are feasible
  - Physics performance, invasive MDI, beam backgrounds
- More complete studies, with full simulation, needed
  - Towards at least four detector proposals to be made by ~2026
    - Light, granular, fast, b and c tagging, lepton ID and resolutions, hadron ID
    - Cost effective
    - Satisfy constraints from interaction region layout

Patrick Janot — FCC-ee workshop: Theory and Experiment, CERN, 7-11 Jan 2019 — 8

https://indico.cern.ch/event/766859/contributions/3252652/attachments/1775501/2887061/FCCeeDiscoveryPotential.pdf

Gelecek Büyük Çaplı Deneyler - II

ILC

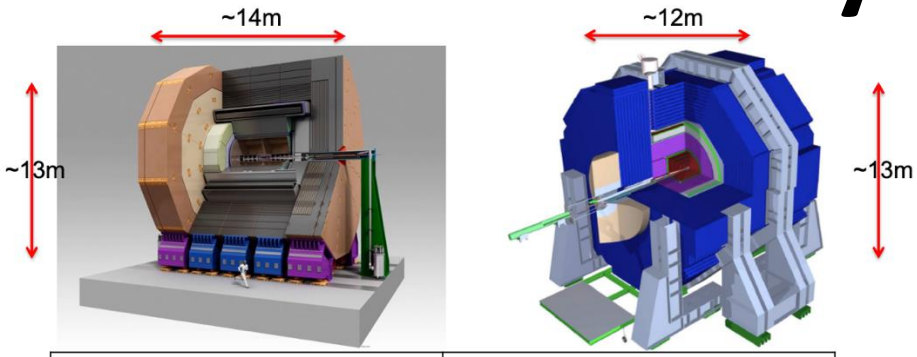

ILD	SiD
Both optimized for PFA PFA Performance ~$B \cdot R_{ECAL,inner}^2$ (two-track separation @ ECAL)	
B = 3.5 T	B = 5 T
$R_{ECAL,inner}$ = 1.8 m	$R_{ECAL,inner}$ = 1.27 m
Si + TPC tracking	Tracking: Si only
Share interaction point via push-pull	

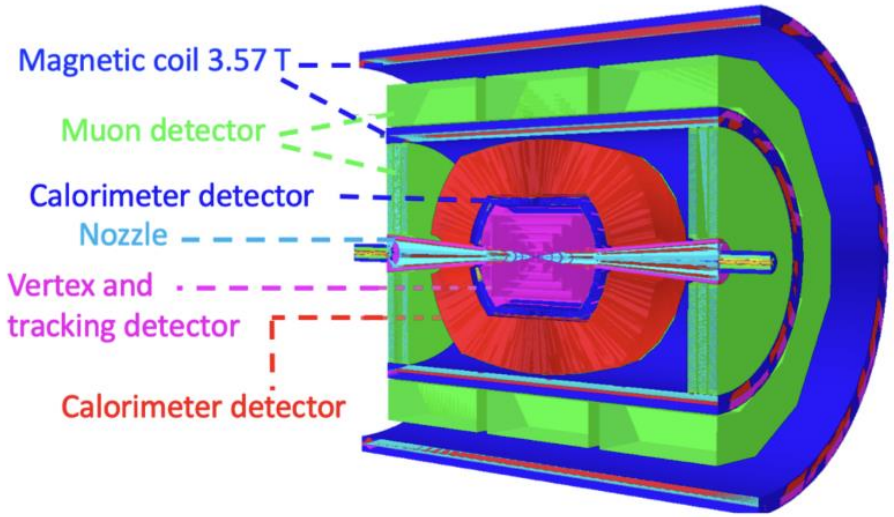

MuCol

CEPC

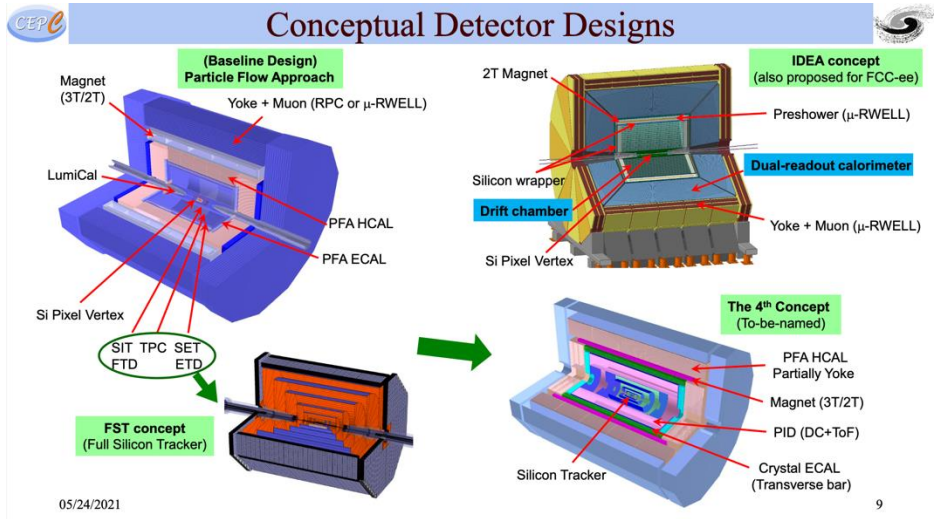

DUNE

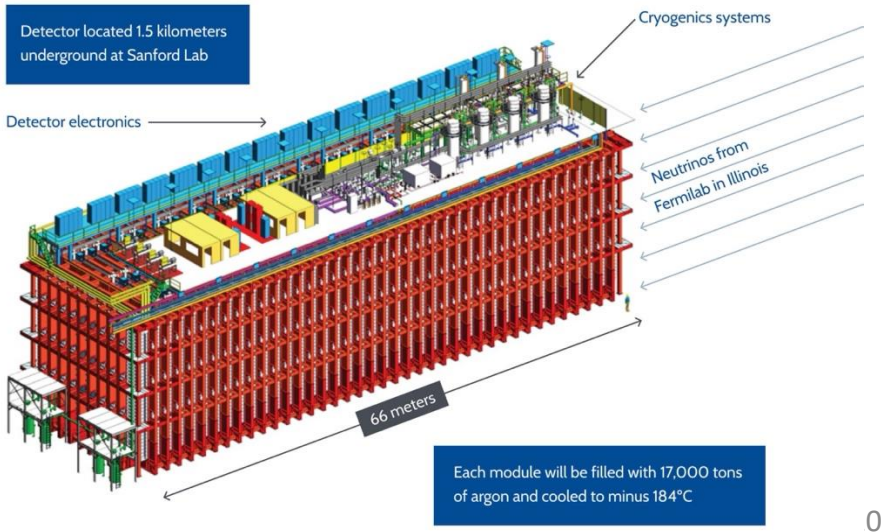

Güncel Dedektör Teknolojileri
ve
Yeni Trendler

Güncel Büyük Çaplı Deneylerin Dedektör Sistemleri

	CMS	ATLAS	ALICE	LHCb
İzci Algıçlar	Silikon	Silikon+Sürüklenme Tüpleri (DT)+TRT	Silikon+Zaman Projeksiyon Odası (TPC)	Silikon+Sürüklenme Tüpleri (DT)
Elektromanyetik Kalorimetre	$PbWO_4$ kristal	Pb/LAr akordiyon	Pb-sintilatör shashlik	Pb-sintilatör shashlik
Hadron Kalorimetresi - Barrel	Brass-scintillator tile	Fe-scintillator tile		Fe-scintillator tile
Hadron Kalorimetresi - Forward	Brass-scintillator tile Fe-quartz fiber	Cu/LAr CuW/LAr	W-quartz fiber	
Muon Sistemi	Sürüklenme tüpleri (DTs) Katot şerit odaları (CSCs) Dirençli levha odaları (RPCs)	Sürüklenme tüpleri (DTs) Katot şerit odaları (CSCs) Dirençli levha odaları (RPCs) Thin Gap Chambers (TGCs)	Katot şerit odaları (CSCs) Dirençli levha odaları (RPCs)	Çok telli orantılı sayaçlar (MWPCs) Gaz elektron çoklayıcılar (GEMs)

Silikon Sensörler

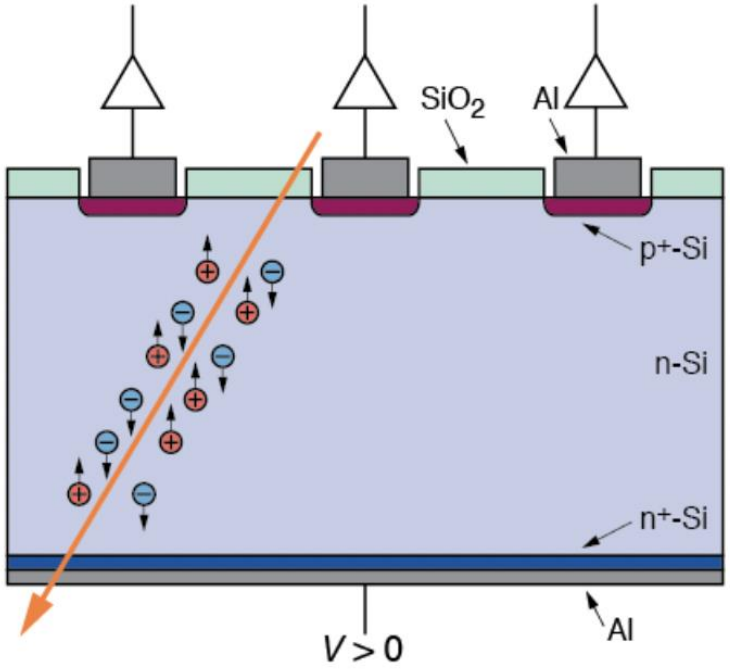

M. Krammer, F. Hartman

https://indico.cern.ch/event/124392/contributions/1339904/attachments/74582/106976/IntroSilicon.pdf

Geçen yüklü parçacıklar, boşalma bölgesinde (depletion region) (standart dedektör kalınlığında yaklaşık 30.000 çift) e-h+ çiftleri oluşturur. Bu yükler elektrotlara doğru sürüklenir. Sürüklenme (akım), her şeride bağlı bir amplifikatör tarafından güçlendirilmiş sinyali oluşturur. Bireysel şeritlerdeki sinyallerden, geçen parçacığın konumu belirlenir.

Standart n-Si şerit sensöründe:

- p+n bağlantısı: $N_a \approx 10^{15}$ cm^{-3}, $N_d \approx 1–5 \cdot 10^{12}$ cm^{-3} (a: acceptor; d: donor)
- n-Si: $\rho > 2$ kΩcm➔ kalınlık 300 µm
- Çalışma voltajı < 200 V.
- Ohmik teması iyileştirmek için arka planda n+ katmanı
- Alüminyum metalizasyon

Silikon Şerit Dedektör Modülü Yapısı

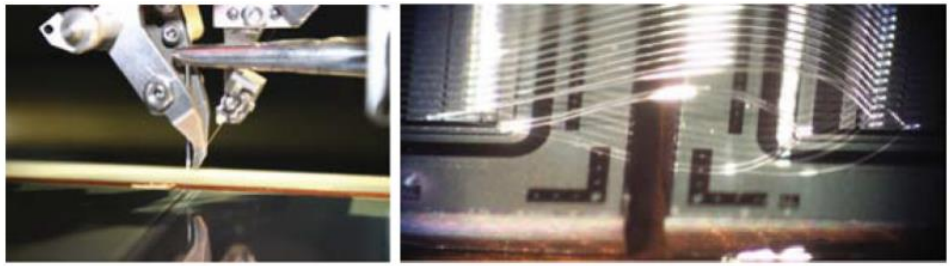

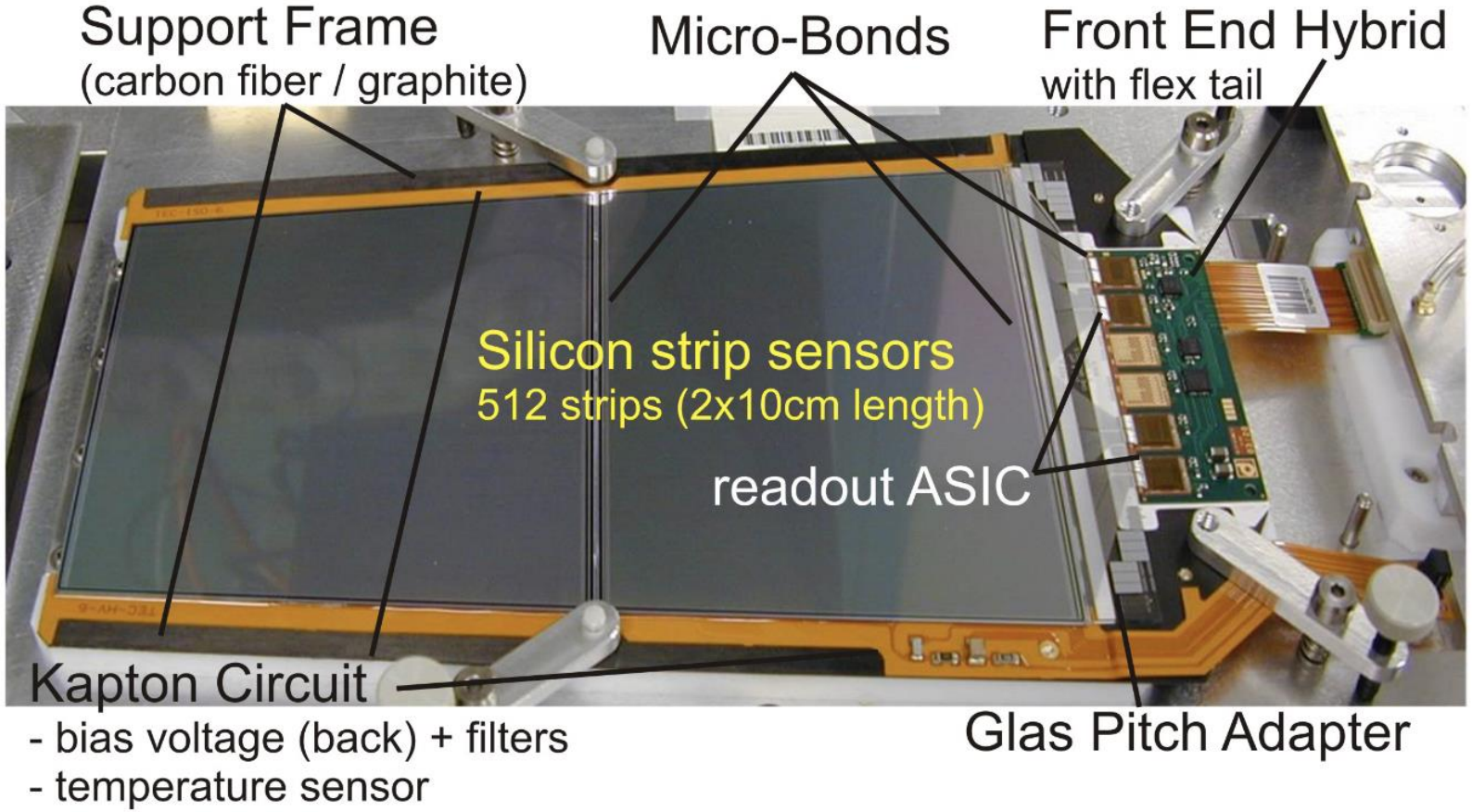

M. Krammer, F. Hartman

https://indico.cern.ch/event/124392/contributions/1339904/attachments/74582/106976/IntroSilicon.pdf

Silikon Sensörlerde Yeni Teknolojiler - I

- **Hibrit Silikon Dedektörler**

Hybrid pixel detectors

Hybrid pixel detectors
- Target applications: CLIC vertex detector, track-timing layers
- Separate interconnected sensor and readout ASIC layers
→ Factorise R&D on sensors and readout ASICs
- Develop new sensor concepts, e.g.:
  - Thin sensors (50 μm) with large fill factor (active edge)
  - Active / passive CMOS sensors
  - Sensors with enhanced lateral drift (ELAD) for optimal position resolution
  - Sensors with charge amplification (LGAD) for picosecond timing
- Profit from advanced industry technologies for highest ASIC performance (rate, timing)
- Profit from synergy with (HL)-LHC developments, medical imaging, gaseous detector r/o (GridPix)
- Refine and develop new interconnect technologies
- Challenges: material budget, interconnect: cost, minimum pitch

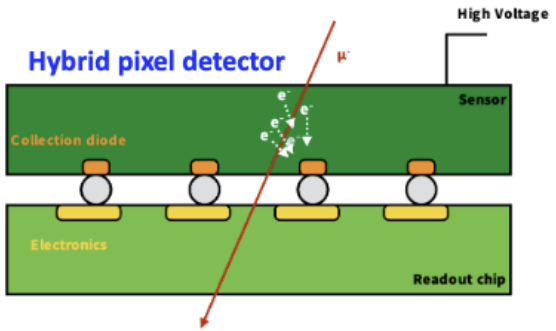

LGAD – Low Gain Avalanche Diodes
<50 ps zaman çözünürlüğü

Hybrid strip detectors

Hybrid strip detectors:
- Baseline for ILC trackers (also suitable for CLIC outer layers)
- Well-established technology (e.g. HL-LHC)
  - low material + power (sparse readout)
  - large and fast signals (dE/dx)
  - high spatial resolution (charge interpolation) in R/phi direction
  - Advanced sensor concepts (e.g. stitched passive CMOS strip sensors)
  - Challenges: not for high occupancy regions; complex interconnect

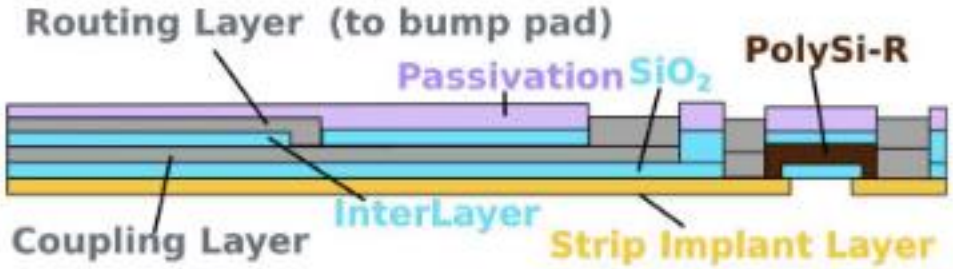

https://indico.cern.ch/event/1232761/contributions/5338927/attachments/2629874/4548397/silicon-sensor-technologies-future-ee-colliders_BTTB11_17Apr2023.pdf

Silikon Sensörlerde Yeni Teknolojiler - II

• SOI – Silicon on Insulator

- Silicon-On-Insulator (SOI): r/o electronics on thin low-resistivity electronics wafer, separated from high-resistivity sensor wafer by buried insulation oxide layer

- Thin + fast (fully depleted) "monolithic" sensors
- Challenge: specialized + complex production process (wafer bonding)
- Various developments targeting LC vertex and tracking detectors, e.g.:
  - SOFIST V1 in 200 nm LAPIS SOI
    20x20 μm² pitch, 200 μm thickness → σ_{SP}~1.4 μm
  - Cracow SOI test chip in 200 nm LAPIS SOI process
    30x30 μm² pitch, 500 μm thickness → σ_{SP}~1.5 μm
  - CPV4 SOI-3D LAPIS SOItest chip (IHEP)
  - IPHC LAPIS SOI test chip (with KEK)
  - 3D developments @ IPHC (with TJ, T-Micro)
- Precision timing not yet demonstrated

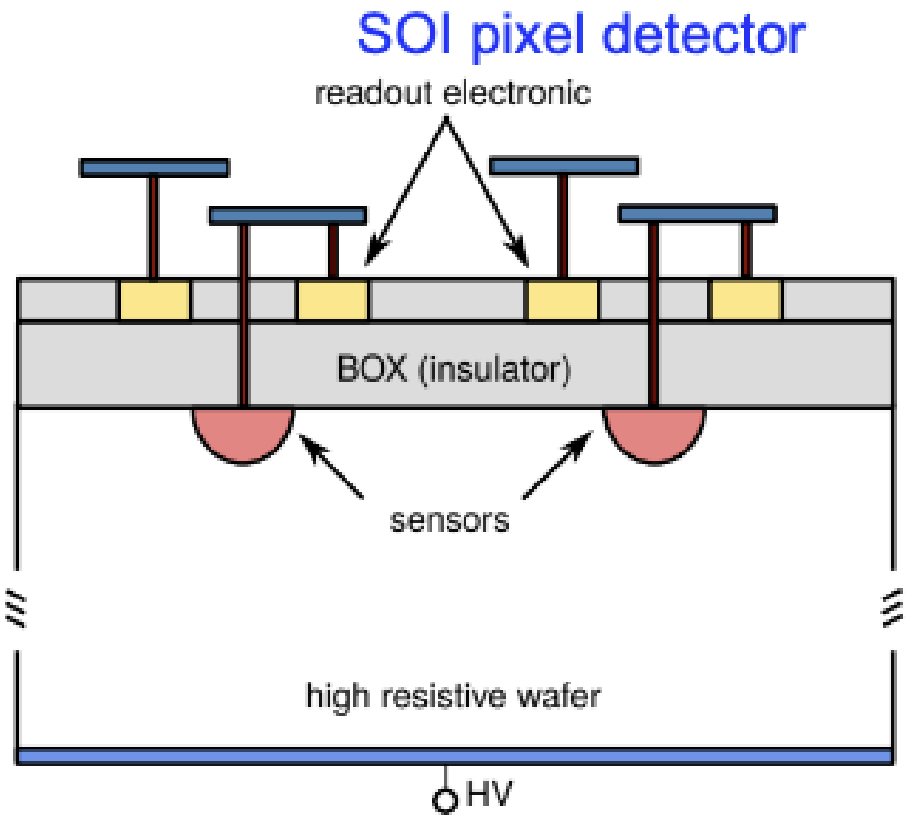

https://indico.cern.ch/event/1232761/contributions/5338927/attachments/2629874/4548397/silicon-sensor-technologies-future-ee-colliders_BTTB11_17Apr2023.pdf

Silikon Sensörlerde Yeni Teknolojiler - III

- **MAPS – Monolithic Active Pixel Sensors**

Significantly lower material budget: sensors and readout electronics are integrated on the same chip

- Eliminate the need for bump bonding : thinned to less than 100µm
- Smaller pixel size, not limited by bump bonding
- Lower costs : implemented in standard commercial CMOS processes

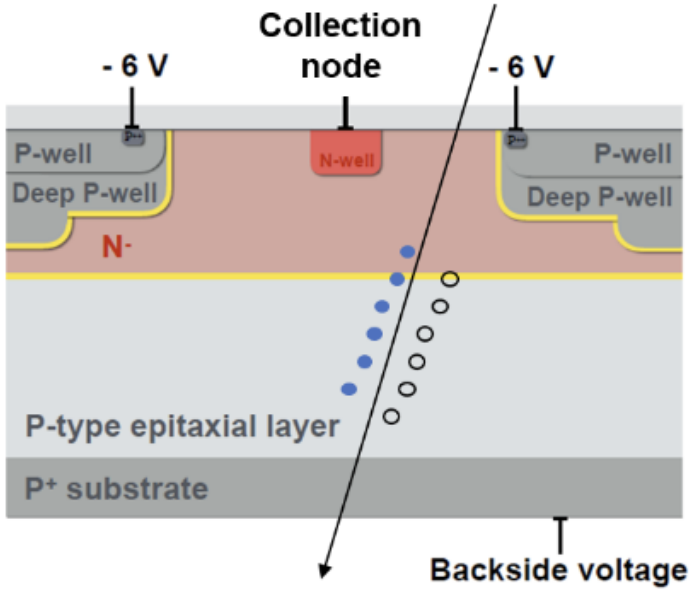

https://indico.fnal.gov/event/22303/contributions/245974/attachments/157387/205863/MAPS.pdf

MAPS Uygulaması

ALICE ITS

The Inner Tracking System (ITS) is the innermost detector of the ALICE central barrel. It consists of seven cylindrical layers all equipped with Monolithic Active Pixel Sensors (MAPS) named ALPIDE (ALice PIxel DEtector).

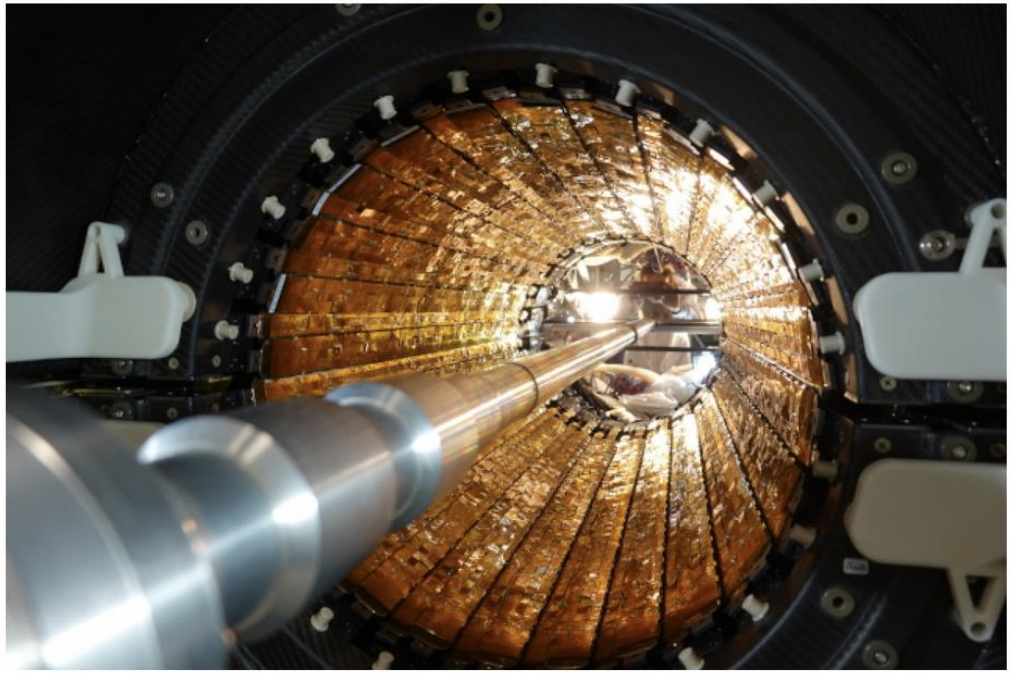

The new detector consists of 7 layers, making it possible to reconstruct tracks based on ITS information alone. With an active area of 10 m^2, segmented in 12.5 billion pixels, **it represents the largest scale application of MAPS in a high-energy physics experiment**. Each ALPIDE chip covers an area of 15x30 mm^2 and contains more than half a million pixels. The performances achieved for power consumption (<40 mW/cm^2) and spatial resolution (~5 micrometer).

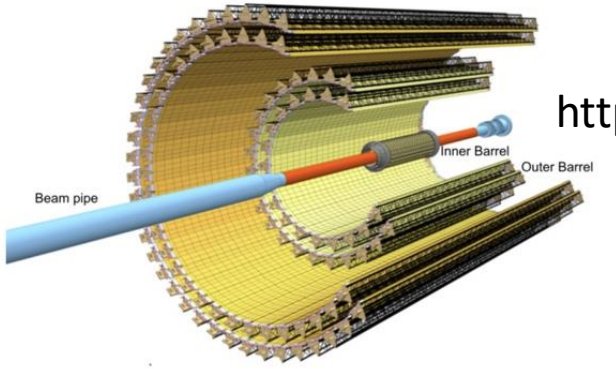

https://arxiv.org/pdf/2111.08301

Gelecek Büyük Çaplı Deneyler İçin Planlanan İzci Dedektör Sistemleri

Collider	ILC		CLIC	FCC-ee			CEPC	
Detector Concept	SiD	ILD	CLICdet	CLD	FCC-ee IDEA	Noble LAr/LKr	CEPC baseline	CEPC IDEA
B-field [T]	5	4	4	2	2	2	3	2
Vertex inner radius [mm]	14	14	31	17 → 12	17 → 12	17 → 12	16	16
Tracker out. radius [m]	1.25	1.8	1.5	2.2	2.0	2.0	1.81	2.05
Vertex	Si-pixel	Si-pixel	Si-pixel	Si-pixel	Si-pixel	Si-pixel	Si-pixel	Si-pixel
Tracker	Si-strips	TPC/ Si-strips	Si-pixel	Si-pixel	DC/ Si-strips	DC/Si-strips or Si-pixel	TPC/Si-strips or Si-strips	DC/ Si-strips

https://indico.cern.ch/event/1232761/contributions/5338927/attachments/2629874/4548397/silicon-sensor-technologies-future-ee-colliders_BTTB11_17Apr2023.pdf

Gazlı Dedektörler

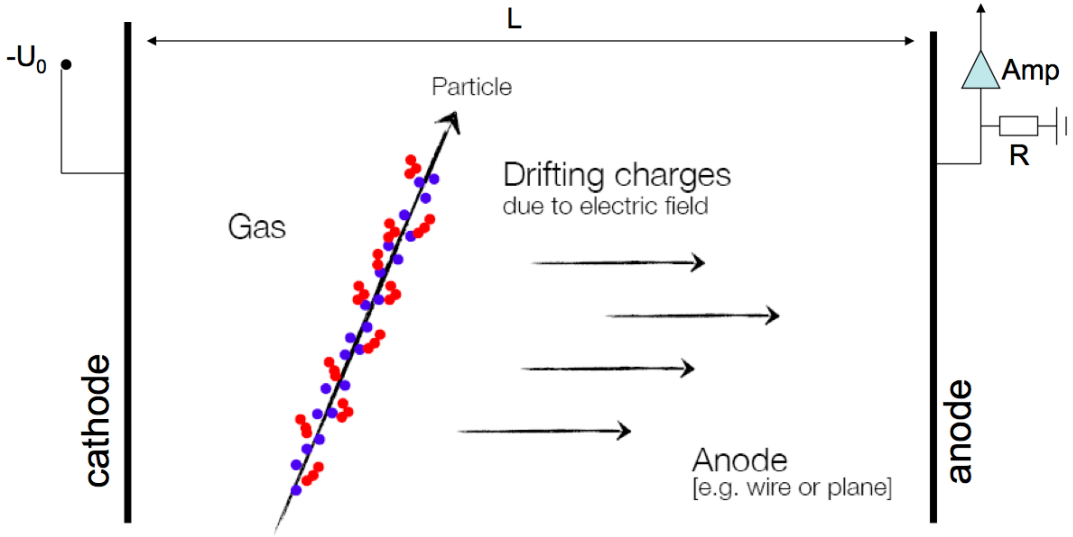

- Primary Ionization
- Secondary Ionization (due to δ-electrons)

Primary ionization

$$X + p \rightarrow X^+ + p + e^-$$

p = charge particle traversing the gas
X = gas atom
e^- = delta-electron (δ)

Secondary ionization

if E_δ is high enough ($E_\delta > E_i$)

$$X + e^- \rightarrow X^+ + e^- + e^-$$

Relevant Parameters
for gas detectors

Ionization energy	:	E_i
Average energy/ion pair	:	W_i
Average number of primary ion pairs [per cm]	:	n_p
Average number of ion pairs [per cm]	:	n_T

Differences due to δ-electrons

$$\langle n_T \rangle = \frac{L \cdot \langle \frac{dE}{dx} \rangle_i}{W_i}$$

[about 2-6 times n_p]
[L: layer thickness]

Typical values: $E_i \sim 30$ eV
$n_T \sim 100$ pairs / 3 keV incident particle

($E_i = I_o$)

Gas	ρ (g/cm³) (STP)	I_0 (eV)	W_i (eV)	dE/dx (MeVg⁻¹cm²)	n_p (cm⁻¹)	n_t (cm⁻¹)
H_2	$8.38 \cdot 10^{-5}$	15.4	37	4.03	5.2	9.2
He	$1.66 \cdot 10^{-4}$	24.6	41	1.94	5.9	7.8
N_2	$1.17 \cdot 10^{-3}$	15.5	35	1.68	(10)	56
Ne	$8.39 \cdot 10^{-4}$	21.6	36	1.68	12	39
Ar	$1.66 \cdot 10^{-3}$	15.8	26	1.47	29.4	94
Kr	$3.49 \cdot 10^{-3}$	14.0	24	1.32	(22)	192
Xe	$5.49 \cdot 10^{-3}$	12.1	22	1.23	44	307
CO_2	$1.86 \cdot 10^{-3}$	13.7	33	1.62	(34)	91
CH_4	$6.70 \cdot 10^{-4}$	13.1	28	2.21	16	53
C_4H_{10}	$2.42 \cdot 10^{-3}$	10.8	23	1.86	(46)	195

Quelle: K. Kleinknecht, *Detektoren für Teilchenstrahlung*, B.G. Teubner, 1992

Ionization mode:
full charge collection
no multiplication; gain ≈ 1

Proportional mode:
multiplication of ionization
signal proportional to ionization
measurement of dE/dx
secondary avalanches need quenching;
gain ≈ $10^4 - 10^5$

Limited proportional mode:
[saturated, streamer]
strong photoemission
requires strong quenchers or pulsed HV;
gain ≈ 10^{10}

Geiger mode:
massive photoemission;
full length of the anode wire affected;
discharge stopped by HV cut

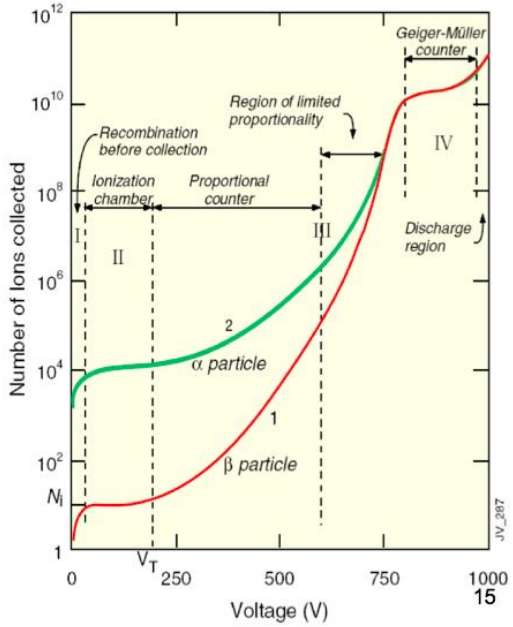

Gazlı Dedektör Örnekleri

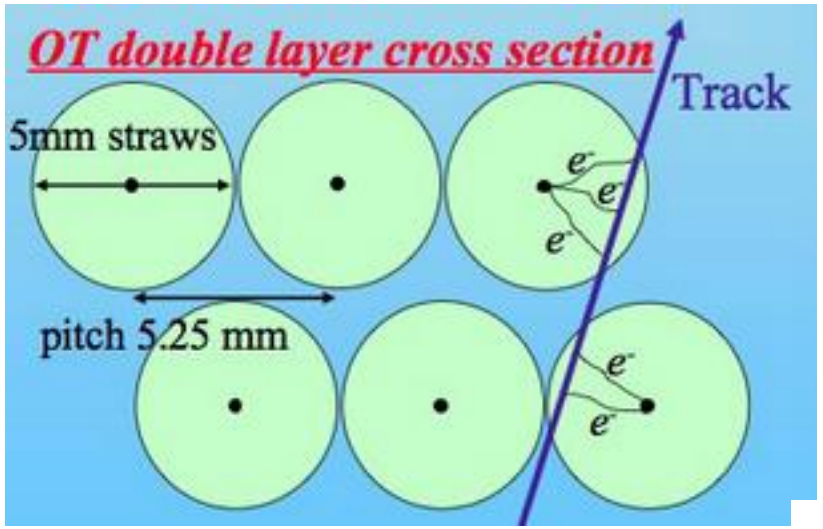

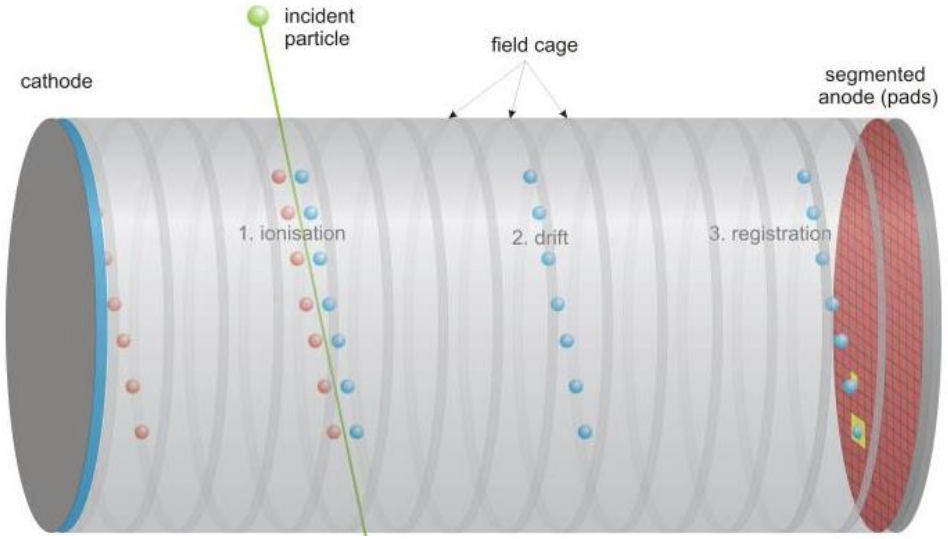

DT
TPC
TRT
RPC
CSC
GEM

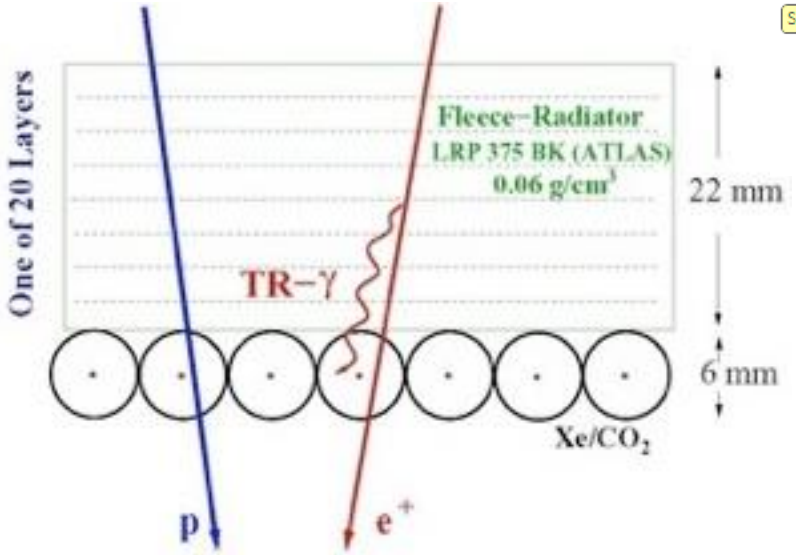

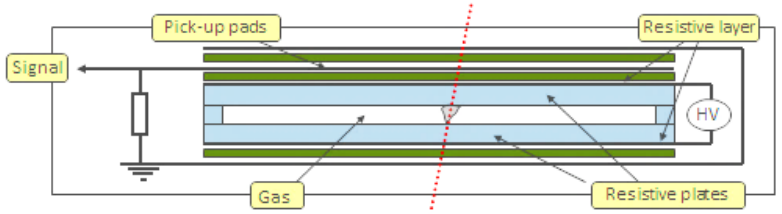

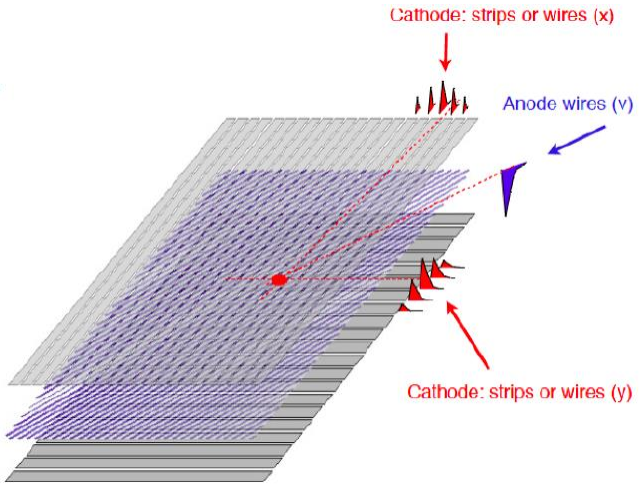

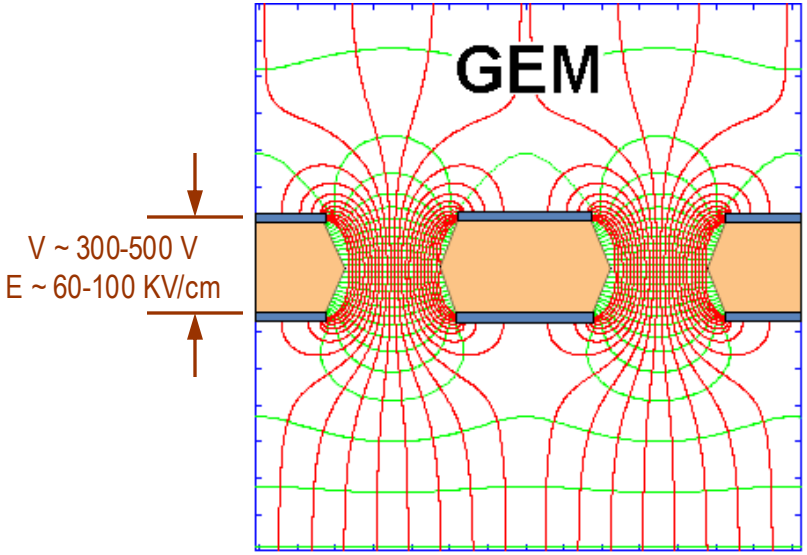

Gazlı Dedektörlerde Yeni Teknolojiler - I

- **Hibrit Gazlı Dedektörler**

Ekibimiz tarafından geliştirilmektedir. Elektron çoğaltım mekanizmasının bir kısmı, gaz katmanından, anot üzerine kaplanan ikincil elektron çoğaltım yeteneği yüksek malzemelere kaydırılır. → fonksiyonel anotlar

Schematic of a hybrid RPC

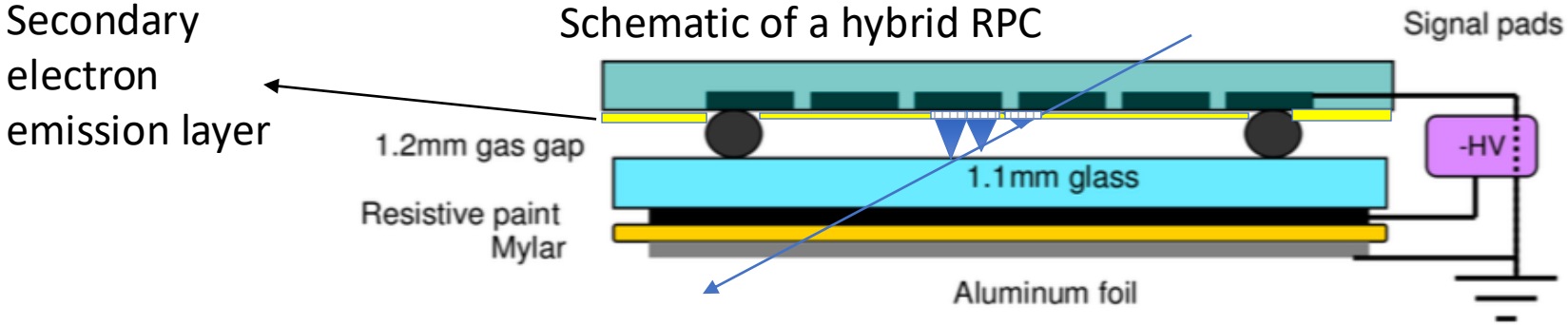

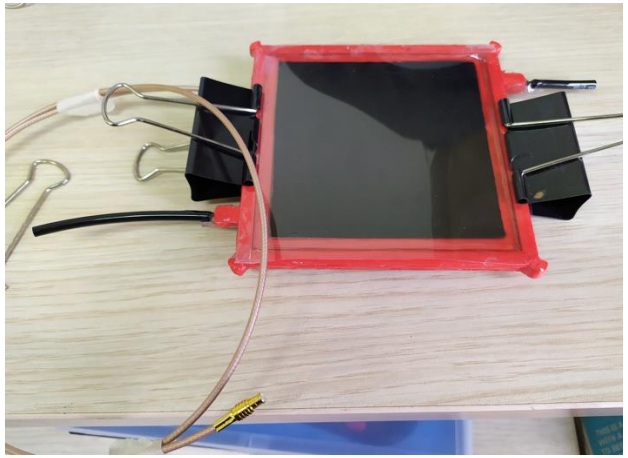

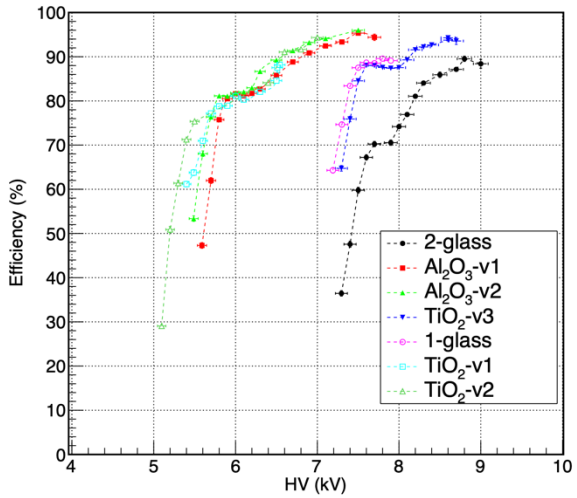

Gazlı Dedektörlerde Yeni Teknolojiler - II

- **(PICOSEC) Micromegas**

PICOSEC detection concept

Precise timing with Micromegas

PICOSEC: Charged particle timing at sub-25 picosecond precision with a Micromegas based detector
J. Bortfeldt et. al. (RD51-PICOSEC collaboration), NIM A (903), 2018, https://doi.org/10.1016/j.nima.2018.04.033

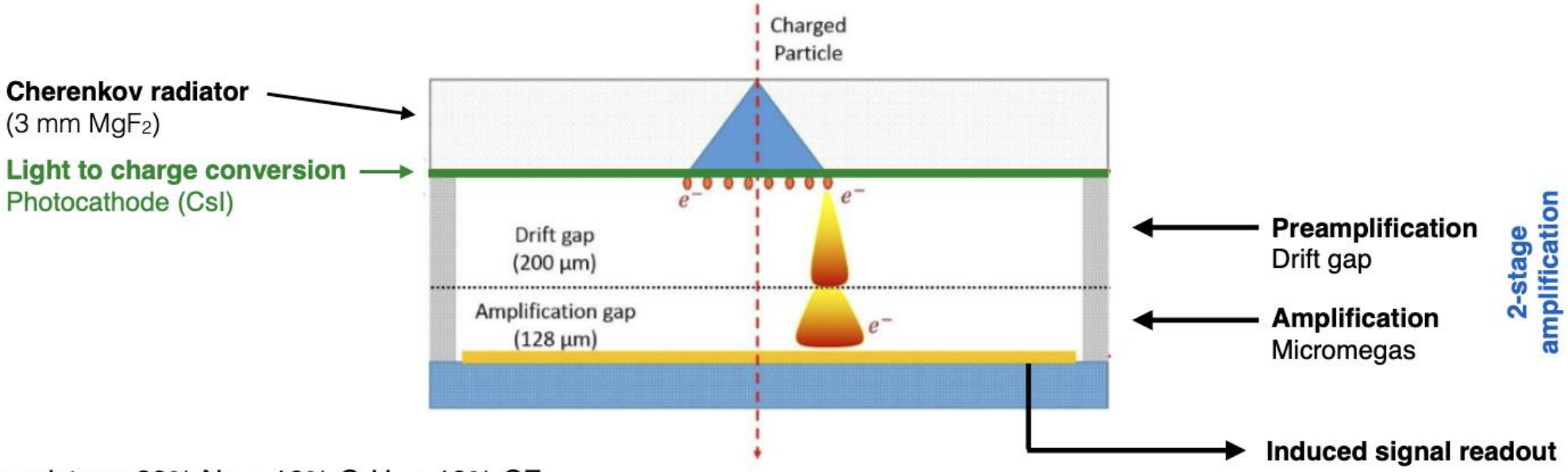

Gas mixture: 80% Ne + 10% C_2H_6 + 10% CF_4
at ambient pressure

Florian M. Brunbauer, IEEE 2024

Gazlı Dedektörlerde Yeni Teknolojiler - III

- **RPWELL, THGEM, µRWELL**

RPWELL

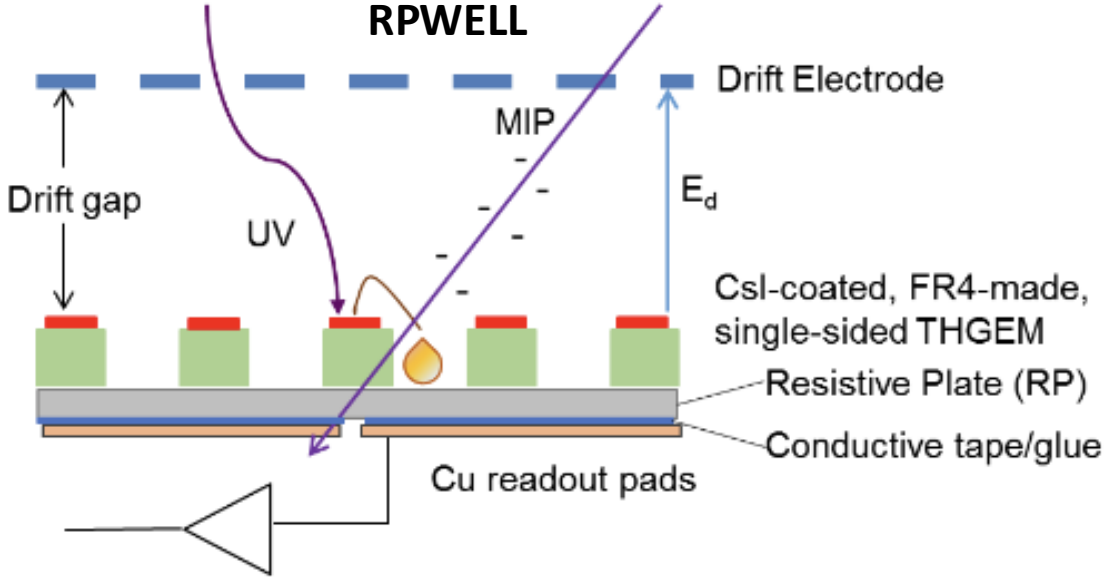

µRWELL

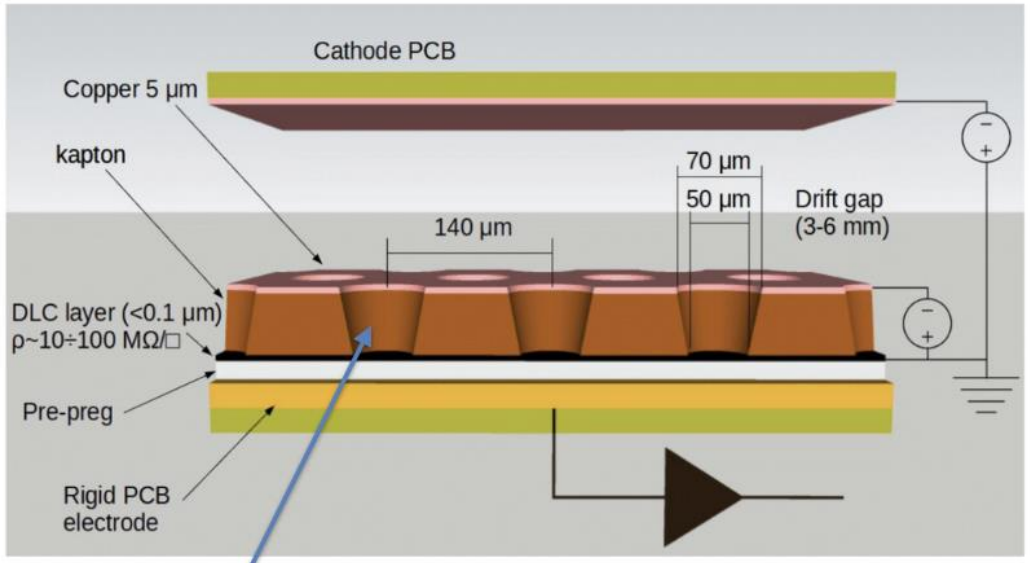

DLC : Diamond-Like Carbon

THGEM

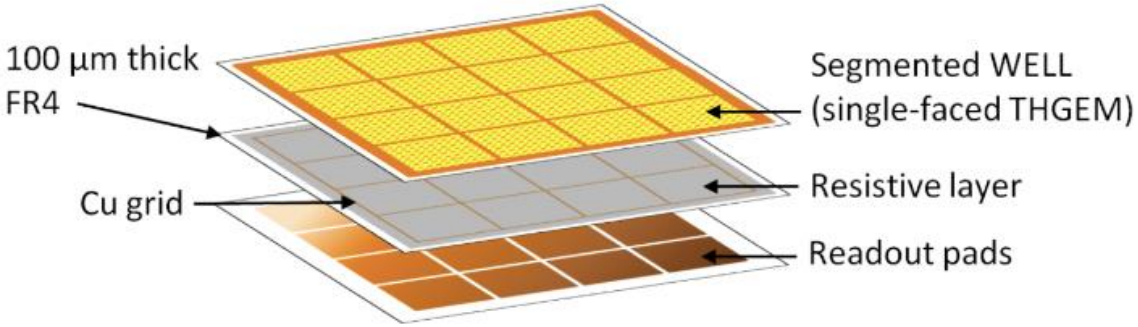

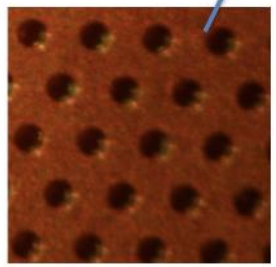

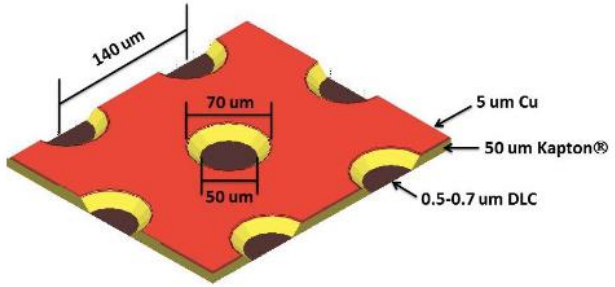

Gazlı Dedektörlerde Yeni Teknolojiler - IV

- **Optik Sinyal Okumalı Gazlı Dedektörler**

Ekibimiz tarafından geliştirilmektedir. Gaz katmanını doğrudan ya da dalga boyu kaydırıcılar sonrasında gören fotodedektörler (SiPM'ler) eşleştirilmiş (hibrit) RPC'ler.

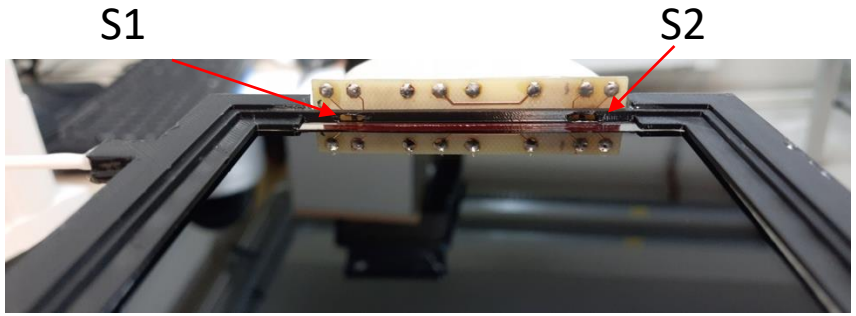

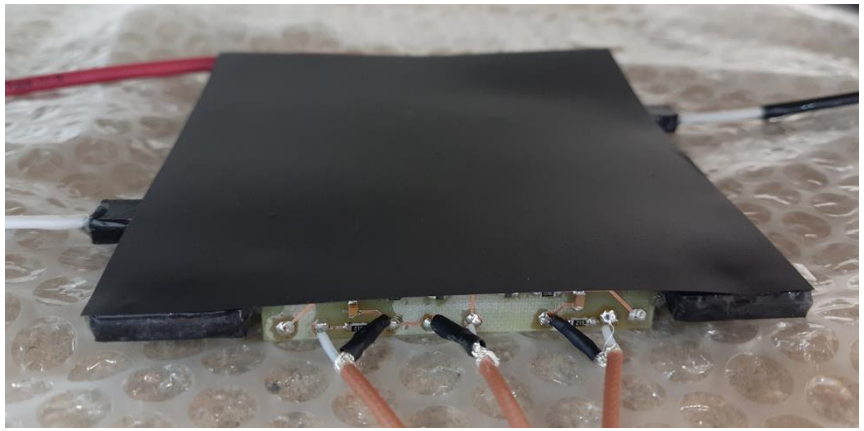

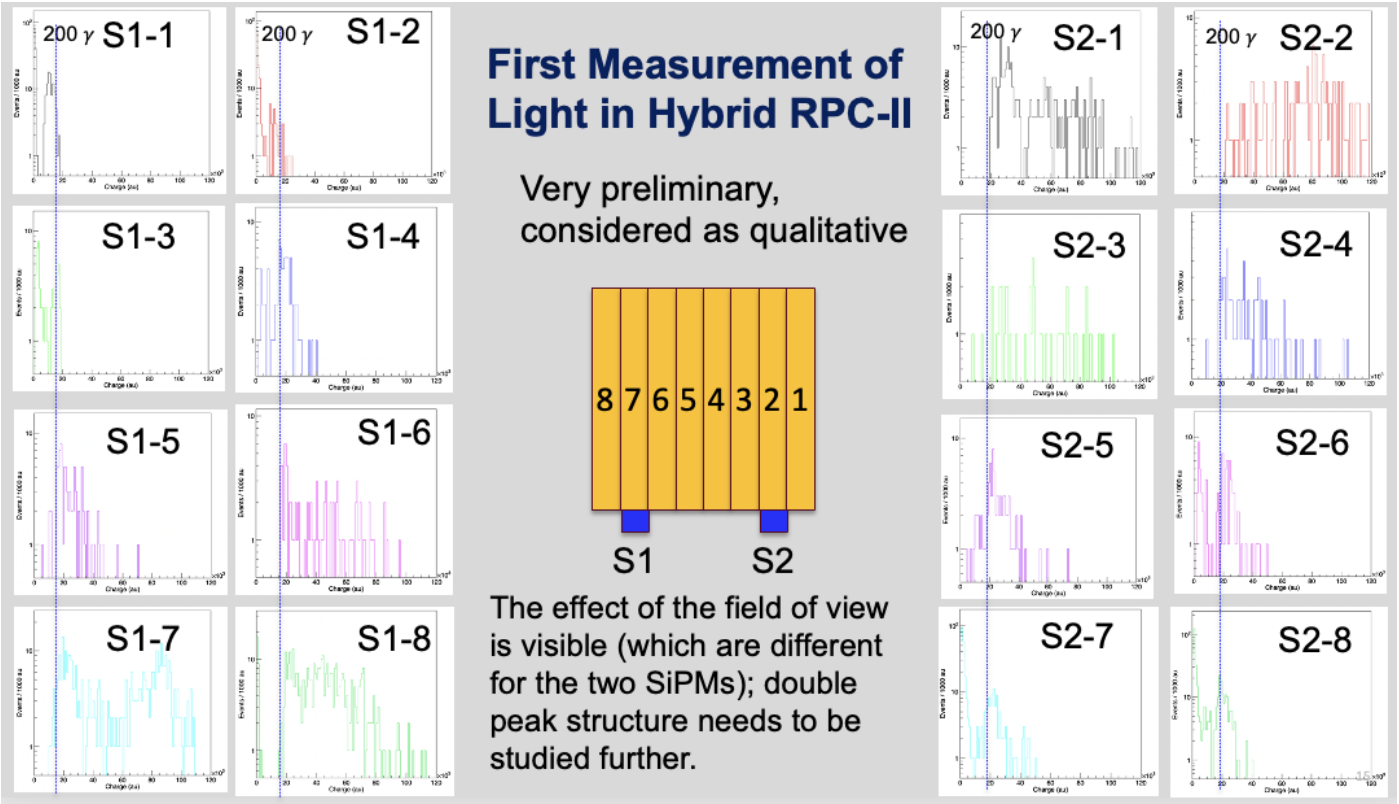

İnorganik Sintilatörlerde Trendler

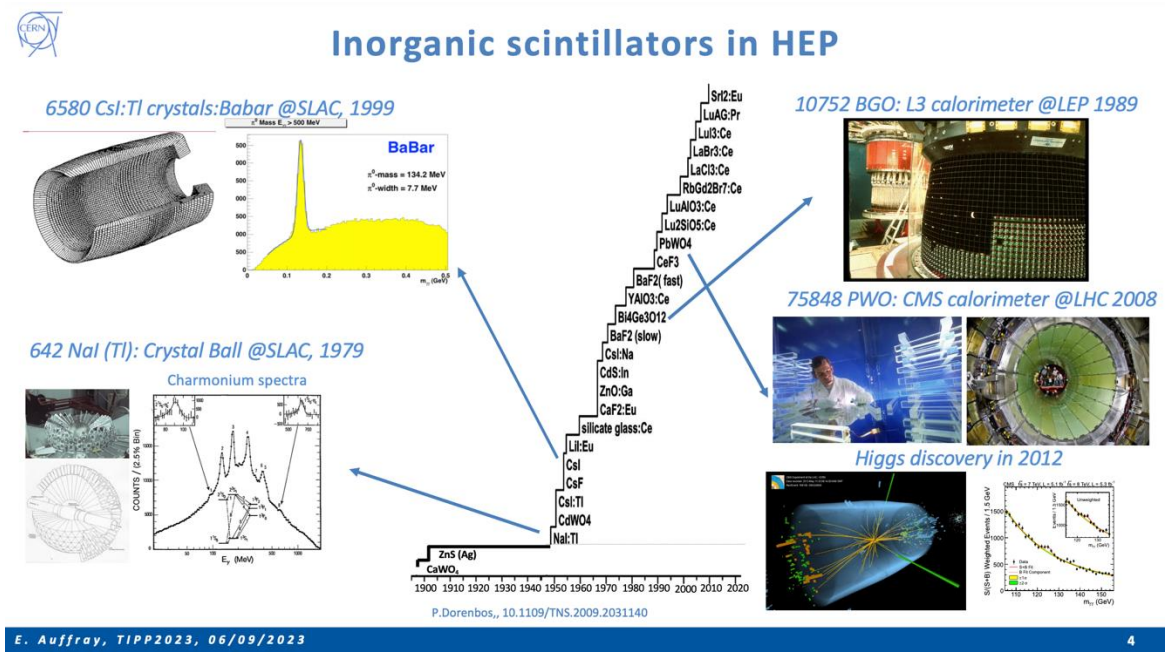

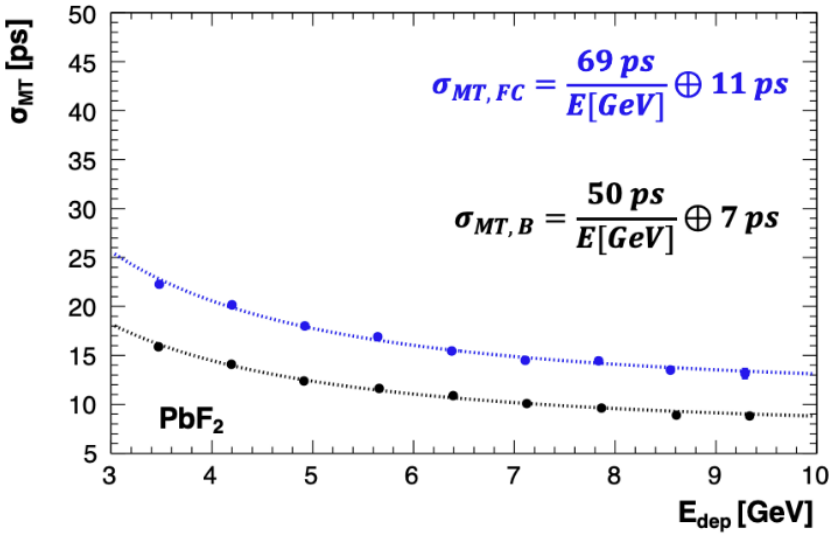

Muon Collider Barrel ECAL Cantone C. et. Al, *Front. Phys.* 11:1223183. doi: 10.3389/fphy.2023.1223183

Inorganic Crystals

Materials:

Sodium iodide (NaI)
Cesium iodide (CsI)
Barium fluoride (BaF_2)
...

Mechanism:

Energy deposition by ionization
Energy transfer to impurities
Radiation of scintillation photons

Time constants:

Fast: recombination from activation centers [ns ... μs]
Slow: recombination due to trapping [ms ... s]

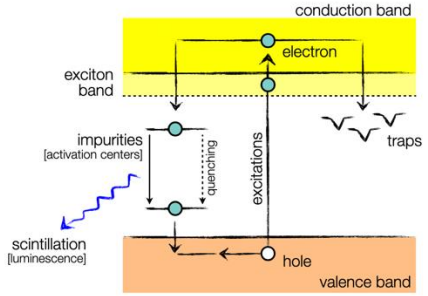

Energy bands in impurity activated crystal showing excitation, luminescence, quenching and trapping

Crystals Used in HEP Calorimeters

Crystal	NaI:Tl	CsI:Tl	CsI	BaF_2	BGO	LYSO:Ce	PWO	PbF_2
Density (g/cm³)	3.67	4.51	4.51	4.89	7.13	7.40	8.3	7.77
Melting Point (°C)	651	621	621	1280	1050	2050	1123	824
Radiation Length (cm)	2.59	1.86	1.86	2.03	1.12	1.14	0.89	0.93
Molière Radius (cm)	4.13	3.57	3.57	3.10	2.23	2.07	2.00	2.21
Interaction Length (cm)	42.9	39.3	39.3	30.7	22.8	20.9	20.7	21.0
Refractive Index[a]	1.85	1.79	1.95	1.50	2.15	1.82	2.20	1.82
Hygroscopicity	Yes	Slight	Slight	No	No	No	No	No
Luminescence[b] (nm) (at peak)	410	550	420 310	300 220	480	402	425 420	-
Decay Time[b] (ns)	245	1220	30 6	650 0.9	300	40	30 10	-
Light Yield[b,c] (photons/MeV)	38,000	63,000	1,400 420	13,680 1,560	8,000	32,000	114 40	-
d(LY)/dT[b] (%/ °C)	-0.2	0.4	-1.4	-1.9 0.1	-0.9	-0.2	-2.5	-
Experiment	Crystal Ball	BaBar BELLE BES III	KTeV Mu2e	TAPS Mu2e-II	L3 BELLE	COMET CMS BTL PIONEER	CMS ALICE PANDA ePIC	A4 G-2

a. at emission peak; b. up/low row: slow/fast component; c. with QE of readout device taken out.

Asal Sıvı Sintilatörler

Scintillation in Liquid Nobel Gases

Materials:

Helium (He)
Liquid Argon (LAr)
Liquid Xenon (LXe)
...

Decay time constants:

Helium : $\tau_1 = .02\ \mu s$, $\tau_2 = 3\ \mu s$
Argon : $\tau_1 \leq .02\ \mu s$

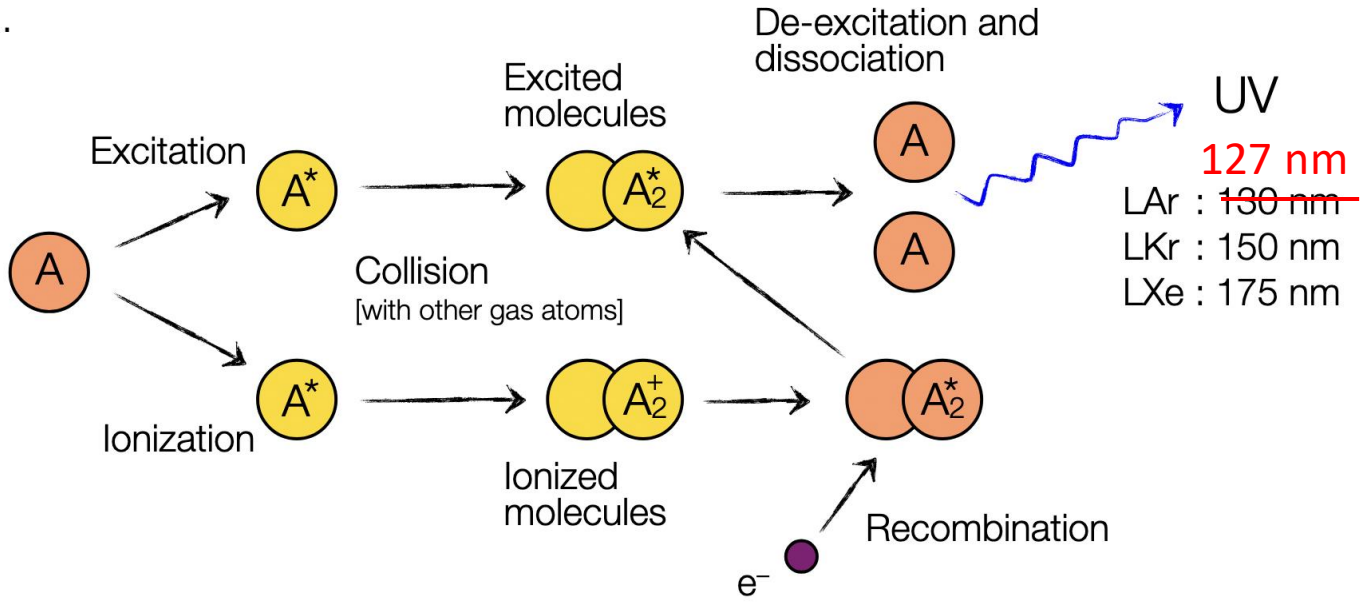

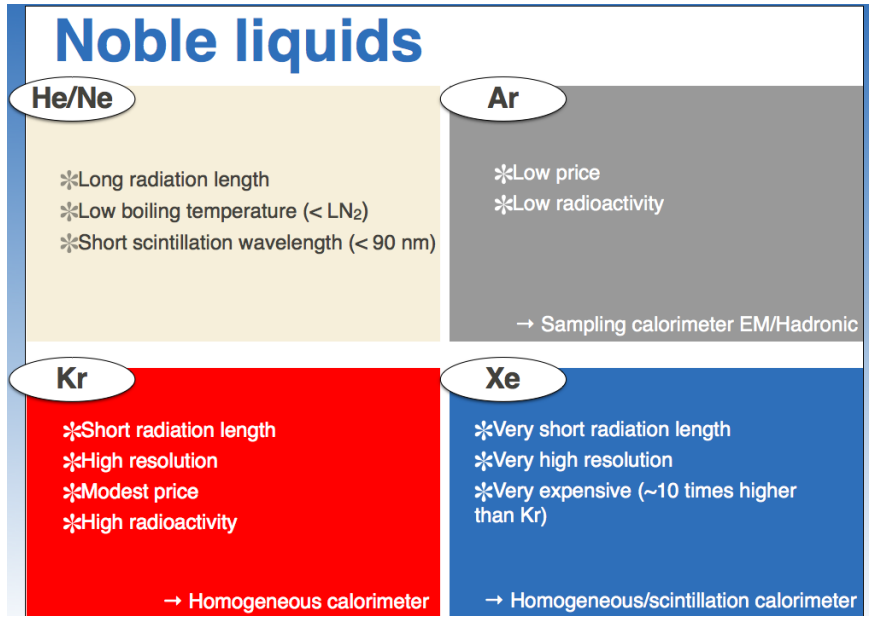

Experiment	Type	Material	Signal	Resolution (%)
D0	Sampling	LAr	Ionization	$16/\sqrt{E} \oplus 0.3 \oplus 0.3/E$
H1	Sampling	LAr	Ionization	$12/\sqrt{E} \oplus 1$
ATLAS	Sampling	LAr	Ionization	$10/\sqrt{E} \oplus 0.4 \oplus 0.3/E$
NA48/62	Homogeneous	LKr	Ionization	$3.2/\sqrt{E} \oplus 0.42 \oplus 0.09/E$
KEDR	Homogeneous	LKr	Ionization	3 @ 1.8 GeV
CMD-3	Homogeneous	LXe	Ionization	$1.78/\sqrt{E} \oplus 1.86$ combined resolution with CsI
MEG	Homogeneous	LXe	Scintillation	1.7 @ 50 MeV

Organik Sintilatörlerde Trendler

Molecular states:

Singlet states
Triplet states

Fluorescence in UV range
[~ 320 nm]

➥ usage of wavelength shifters

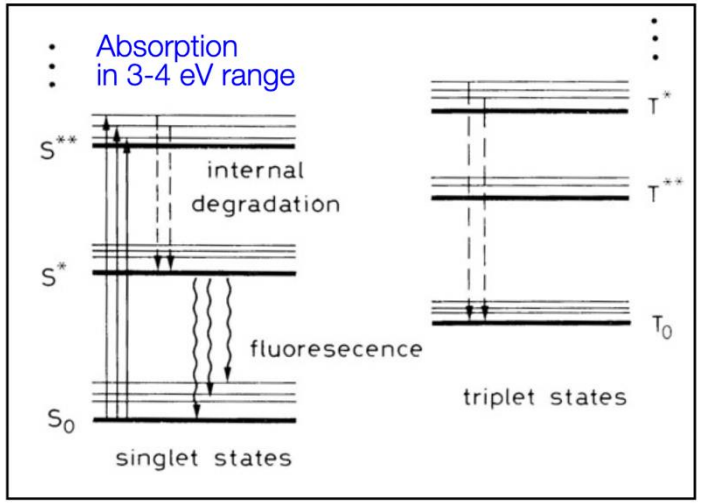

Fluorescence : $S_1 \rightarrow S_0$ [< 10^{-8} s]
Phosphorescence : $T_0 \rightarrow S_0$ [> 10^{-4} s]

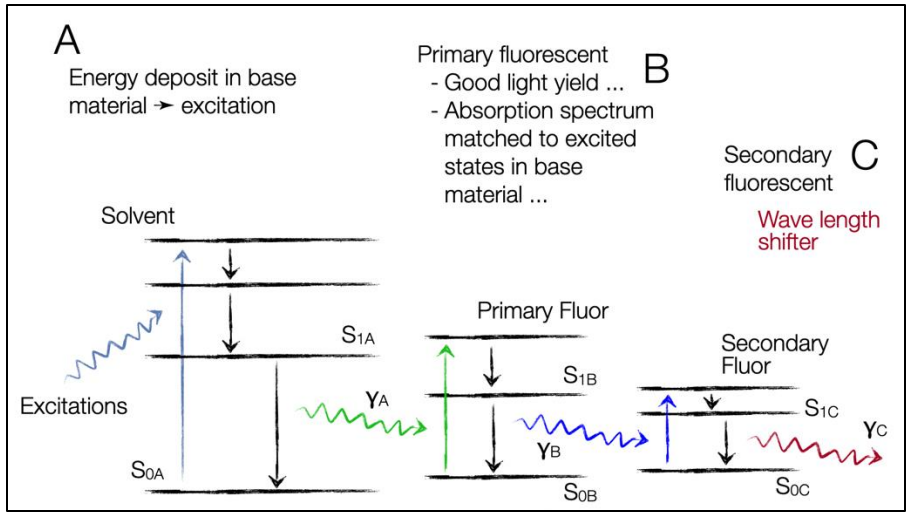

our nanocomposite samples produced @ UniMiB

$PVT/DVB_{90/10\%} + PTP_{\alpha} + \gamma^{*}:CsPbBr_{3\beta} + perylene\ dyad_{\delta}^{\dagger}$

	α	β	γ*	δ	optical features (visual inspection)
Blank_0	0	0	-	0	transparent, colourless
Blank_1	1.5%	0	-	0	transparent, colourless
Blank_2	0	0	-	> 0	transparent, orange
Blank_3	1.5%	0	-	> 0	transparent, orange
NC23_2	1.5%	1.5%	Yb	0	a bit opaque, green
NC23_4	1.5%	1.5%	Yb	>0	a bit opaque, orange
NC24_0	0	1.5%	F	0	opaque, green
NC24_1	0	2.5%	F	0	very opaque, green
NC24_2	1.5%	1.5%	F	0	opaque, green
NC24_3	0	1.5%	F	>0	very opaque, orange
NC24_4	1.5%	1.5%	F	>0	very opaque, orange

CALOR 2024 Mattia Soldani 10

- surface passivation to allow use of perovskite in thermally polymerised matrix

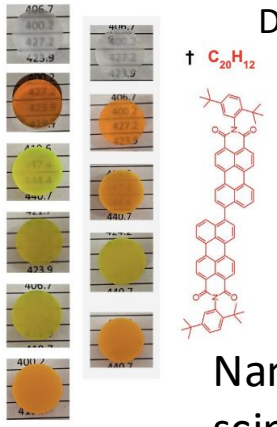

DVB: Divinylbenzene

Nanocrystal-based scintillators

https://indico.cern.ch/event/1339557/contributions/5898478/attachments/2860074/5003725/24_05_21_calor_nanocal_soldani.pdf

İSÜ Gd Katkılı PS'lerin Doğrusallığı

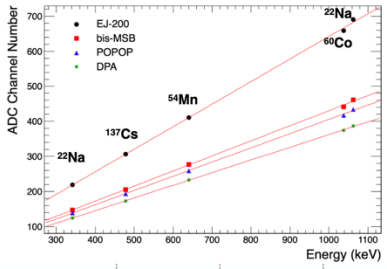

- ☑ Gd katkılı PS örnekleri iyi bir doğrusallığa sahip.
- ☑ Göreli ışık çıktısı EJ-200 ile kıyaslanabilir seviyede.
- ☑ bis-MSB en yüksek göreli ışık çıktısı sağlıyor.

$R_{sample} = R_{EJ-200} \times V_{CE,sample}/V_{CE,EJ-200}$

Samples	^{22}Na	^{137}Cs	^{54}Mn	^{60}Co	^{22}Na	Rel. LY @ 80%
EJ-200	100	100	100	100	100	100
bis-MSB	67.63	66.86	67.33	67.03	66.84	67.14 ± 0.14
POPOP	63.77	63.06	63.14	63.35	62.84	63.23 ± 0.14
DAP	57.00	56.29	56.51	56.72	55.88	56.48 ± 0.17

8 Sertac Ozturk

https://indico.global/event/1464/contributions/28326/attachments/14427/22453/DetectorArge_Sertac_2024.pdf

Cerenkov Işıması Radyatörleri

Super-Kamiokande

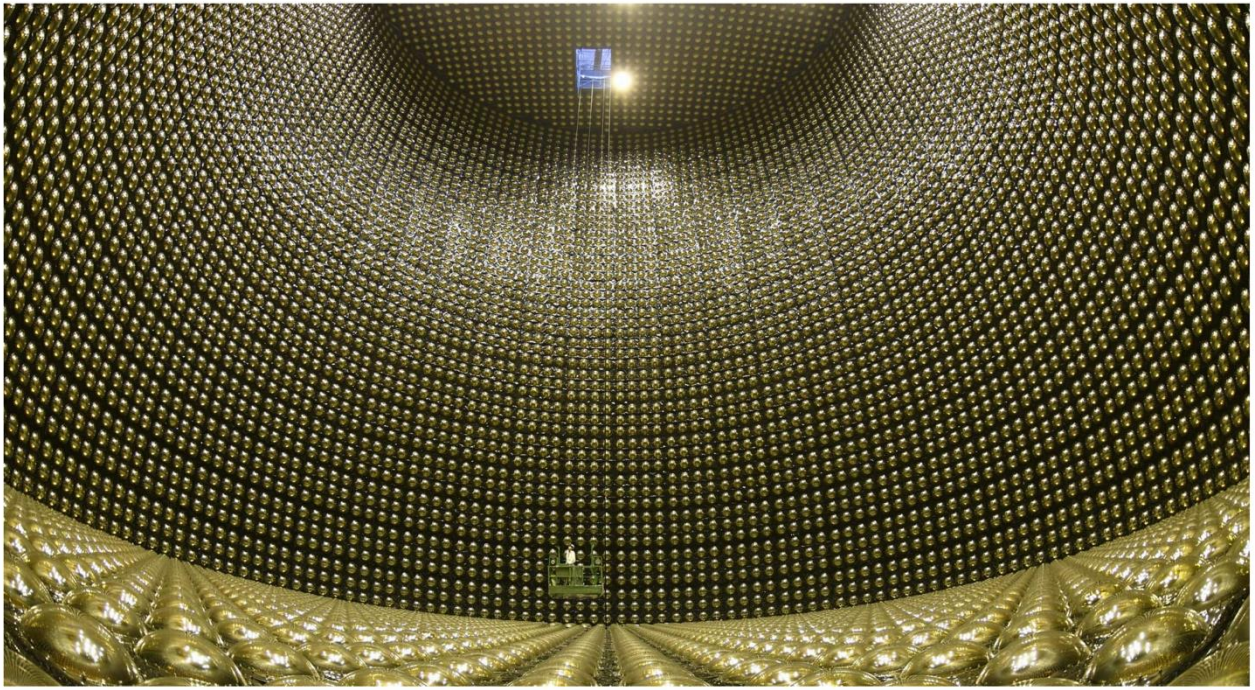

Super-Kamiokande is the world's largest water Cherenkov detector. It consists of a stainless-steel tank, 39.3m diameter and 41.4m tall, filled with 50,000 tons of water. About 13,000 photo-multipliers are installed on the tank wall. The detector is located at 1,000 meter underground in the Kamioka-mine, Hida-city, Gifu, Japan.

The RICH system has the task of identifying charged particles over the momentum range 1-150 GeV/*c*, within an angular acceptance of 10-300 milliradians (mrad).

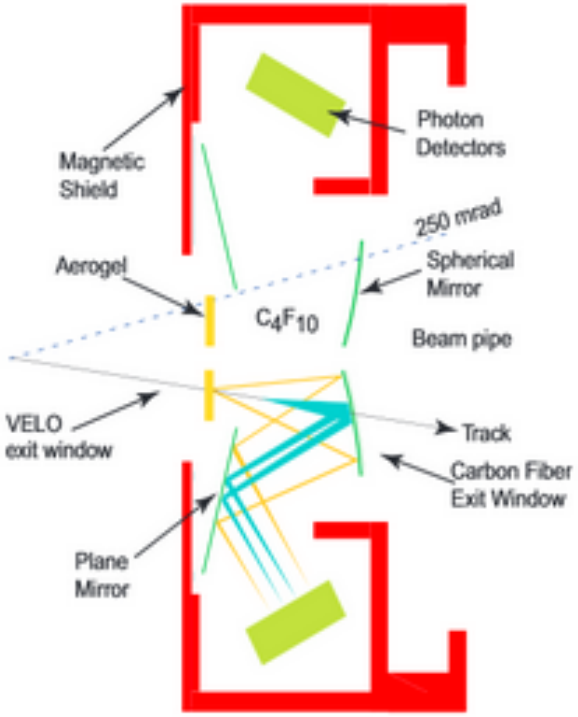

The system consists of an upstream detector (RICH-1) with silica aerogel and C_4F_{10} gas radiators, positioned directly behind the VELO, and a downstream detector (RICH-2) with a CF_4 gas radiator, located behind the magnet and the tracking system.

C_4F_{10} : perfluorobutane

CF_4 : carbon tetrafluoride

Cerenkov Işıması Radyatörleri Yeni Teknolojiler

Introduction to ARC

- The Array of RICH Cells (ARC) detector provide PID capabilities for FCC-ee detector with a small radial extent (20 cm) and a minimal impact on material budget (<0.1X_0)

Detector description of ARC

- The **ARC** consists of an large array of independent **RICH cells** placed as in the picture below (only mirrors and sensors are visible for simplicity)
- Each RICH cell consists of an spherical mirror (1) which focuses the light produced in the two Cerenkov radiators (2,3) into a light sensor (4)
- **CLD option 3** has a smaller tracker to fit ARC. See G. Sadowski study about the tracking performance of this CLD option (EPJ-WoC)

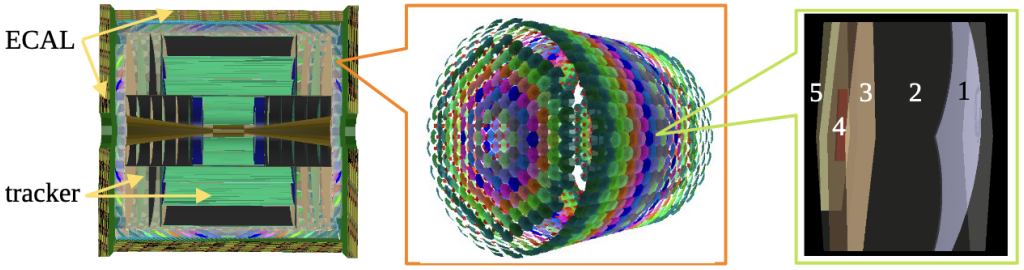

CLD option 3 ARC RICH cell

Working principles of ARC

- There are two Cerenkov radiators inside each RICH cell, a gas and an aerogel
- When a charged particle crosses a cell, two cones of Cerenkov photons are created. The detected photon energy is in the range of (2, 6) eV, or (200, 600) nm
- The hit pattern in the sensor corresponds to two concentric rings
- DD4hep and Geant4 are used to simulate the behavior of the ARC detector

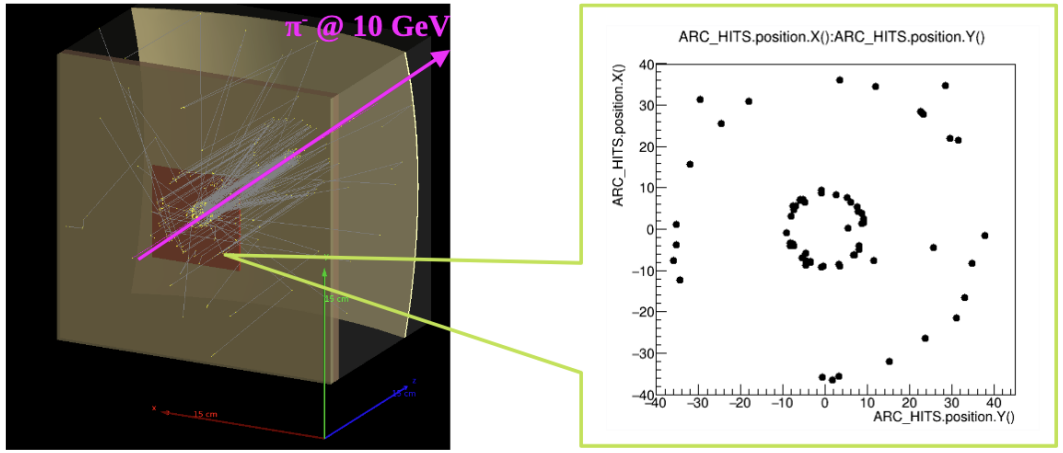

https://indico.cern.ch/event/1439509/contributions/6298368/attachments/2996481/5279241/fccphysweek25_ARC_atd_v3.pdf

Fotodedektörler

Fotoçoğaltıcı Tüp (PMT)

- ☑ Işığı elektrik akımına çevirir.
  - ✦ Katota çarpan ışık fotoelektrik etki ile elektron koparır.
  - ✦ Dinotlara çarpan elektronlarda ikinci elektronlar üretir.
  - ✦ En son anota bir elektron duşu ulaşır.
- ☑ Çeşitli şekil ve boyutlarda olabilirler.
- ☑ Yüksek voltaj gerektirir (1200-1700 V)
- ☑ Kazanç, kuantum verimlilik, sinyal zamanı, karanlık akım önemli parametrelerdir.

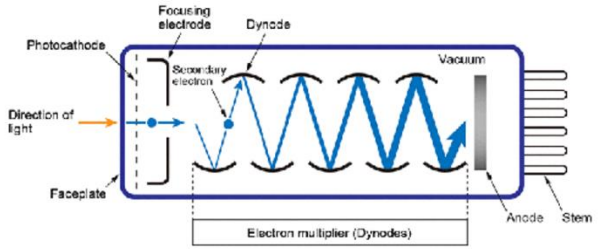

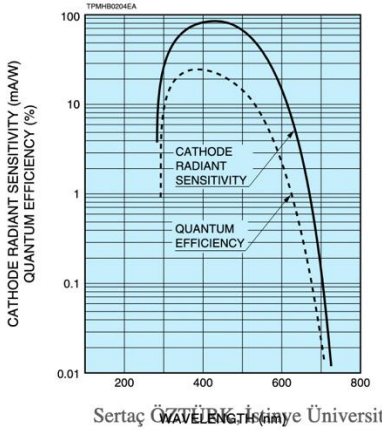

Silikon Fotoçoğaltıcı

SiPM

- ☑ Işığı elektrik akımına çevirir.
  - ✦ Yarı iletken
- ☑ Piksellerden meydana gelir.
  - ✦ 1000 piksel/mm2
- ☑ Yüksek kazanç, hızlı zaman tepkisi
- ☑ Düşük çalışma voltajı
- ☑ Manyetik alandan etkilenmez.
- ☑ Küçük yüzey alanı.

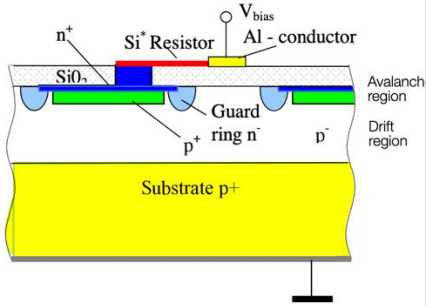

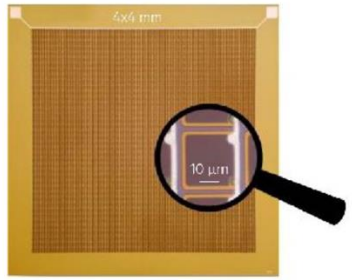

Micro Channel Plate

MCP

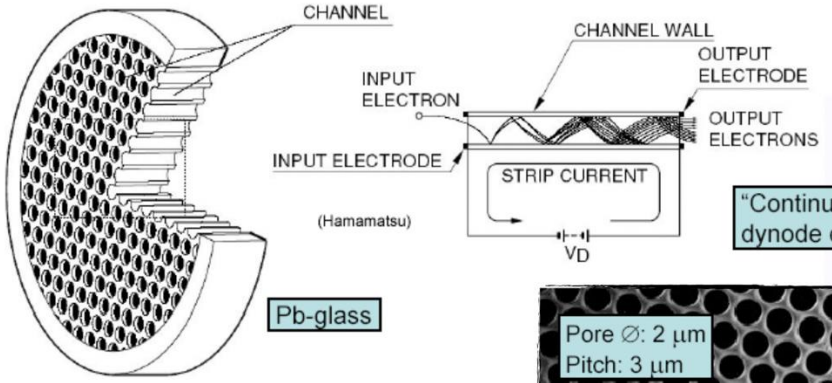

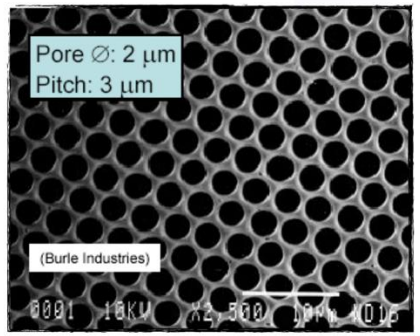

"2D Photomultiplier"

Gain: $5 \cdot 10^4$
Fast signal [time spread ~ 50 ps]
B-Field tolerant [up to 0.1T]

But: limited life time/rate capability

Fotodedektörlerde Yeni Trendler

* Daha çok SiPM! (240.000 CMS-HGCAL)

* Sıvı Argon uyumlu (127 nm duyarlı) SiPM'ler
* LAPPD

Measurement wavelength	Academic research	Measuring instruments (flow cytometers, microscope etc.)	PET scanners	LiDAR
VUV/UV	For academic research experiments			
VIS	For wide dynamic range S14160 series		For PET scanners S14160/S14161 series	
	For precision measurement S13360/S13362 series			
	For precision measurement (TSV type) S13360/S13361/S13363 series			
VIS to NIR		For visible light S14420/S14422 series		
NIR				For near infrared S15639/S16786 series

https://www.hamamatsu.com/eu/en/product/optical-sensors/mppc/mppc_mppc-array.html

Enabling the vision of tomorrow through experimental scientific discovery.

Incom's LAPPD™ is the world's largest and fastest MCP based photodetector. With picosecond level timing, high spatial resolution and the industry's lowest dark counts, no detector is more capable of imaging with single photon sensitivity. Our LAPPD™ was developed in partnership with the Department of Energy, Argonne National Labs, and the University of Chicago to explore the elementary constituents of matter and energy, the interactions between them, and the nature of space and time. After nearly ten years of development, Incom is proud to bring this revolutionary technology to market.

FEATURES

- Large area 200 mm x 200 mm
- Quantum Efficiency > 20% (90% uniformity)
- Chevron pair of 203 mm x 203 mm ALD-GCA-MCPs
- Gain > 1 x 10^7
- Independent control of voltage to the photocathode and MCPs
- High temporal resolution
- 1mm Spatial resolution
- Dark count rate less than 150 Hz/s/Cm^2

APPLICATIONS

- High energy physics
- Nuclear physics
- Medical imaging (PET)
- Neutron detection
- Neutrino interaction

20 CM SQUARE LAPPD™

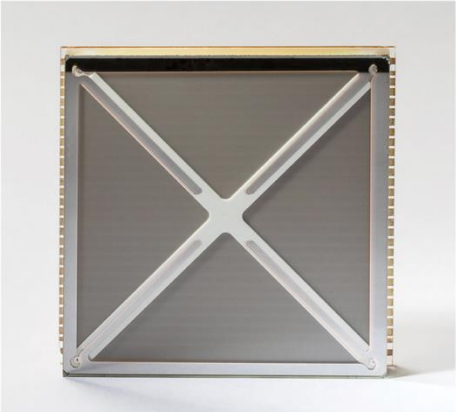

https://incomusa.com/lappd/

Yük Okuma Elektroniği

• Detector signal generally a short current pulse:

i =V/R (R = 50Ω, oscilloscope termination)

– thin silicon detector (10 –300 μm): 100 ps–30 ns
– thick (~cm) Si or Ge detector: 1 –10 μs
– proportional chamber: 10 ns –10 μs
– Microstrip Gas Chamber: 10 –50 ns
– Scintillator+ PMT/APD: 100 ps–10 μs

$$E \propto Q_s = \int i_s(t)dt$$

Various measurements of this signal are possible
Depending on information required:

- Signal above threshold
  digital response / event count
- Integral of current = charge
  ➔ energy deposited
- Time of leading edge
  ➔ time of arrival (ToA) or time of flight (ToF)
- Time of signal above threshold
  ➔ energy deposited by TOT

and many more …

oscilloscope picture

https://www.desy.de/~garutti/LECTURES/ParticleDetectorSS12/L8_readoutElectronics.pdf

Yük Okuma Elektroniği Standart Trend - ASIC

Most front-ends follow a similar architecture

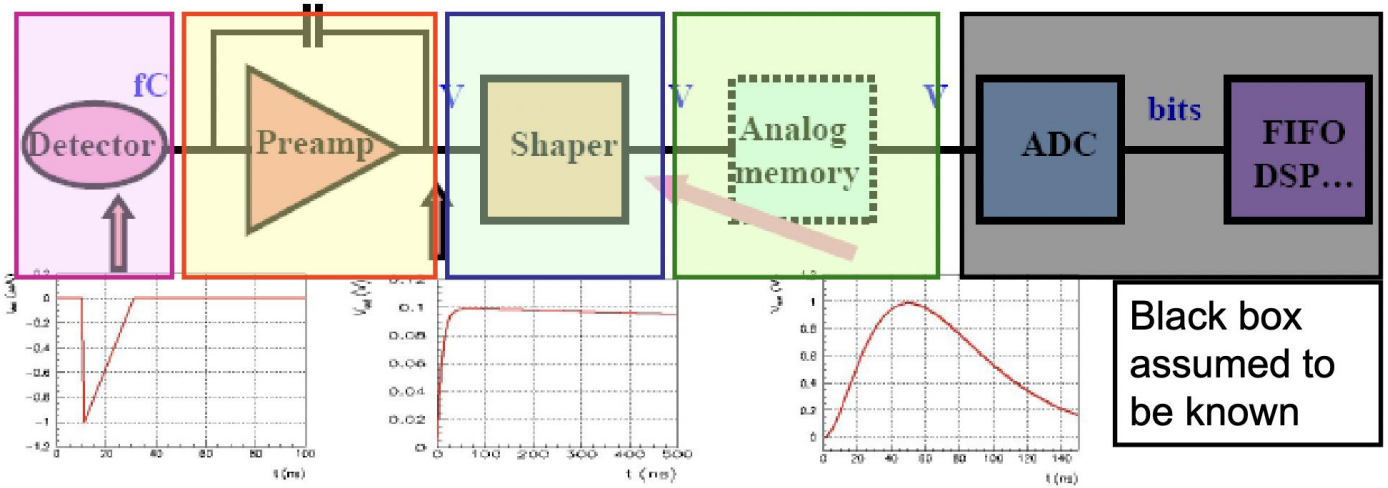

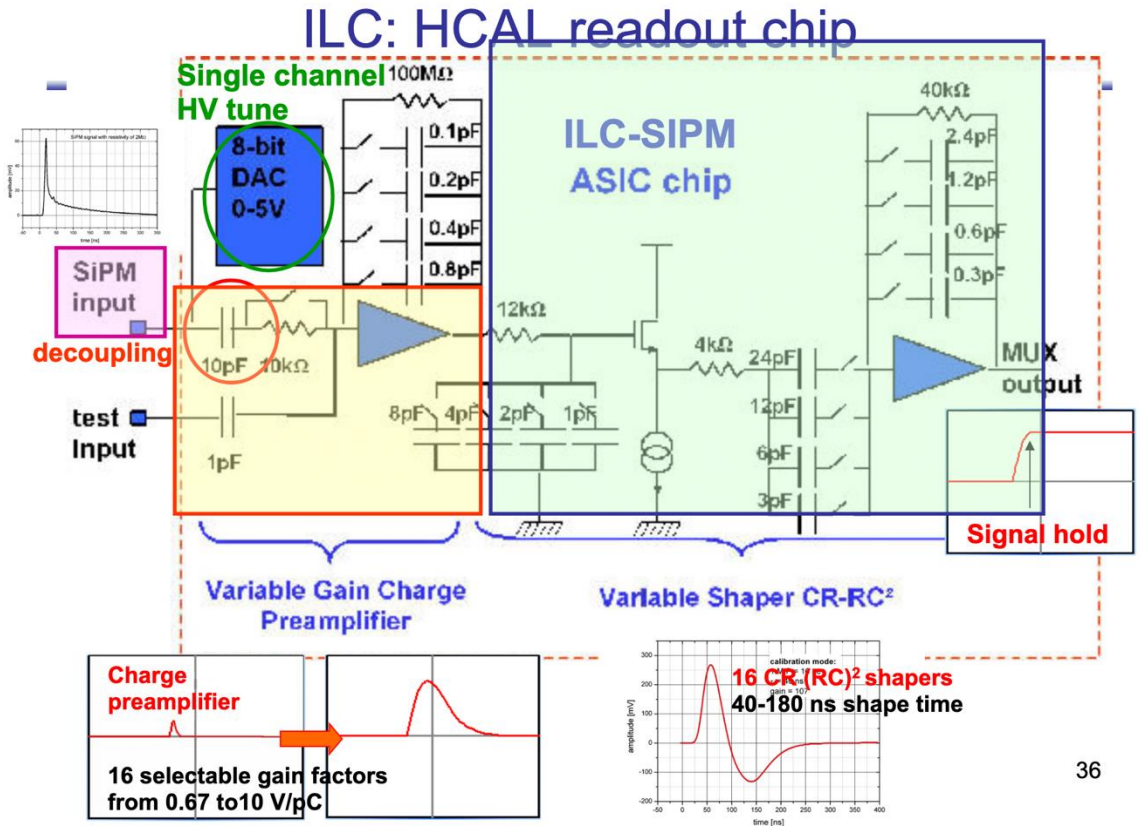

- Very small signals (fC) -> need amplification
- Measurement of amplitude (ADC)
- Thousands to millions of channels

Daha hassas, daha fonksiyonel, daha hızlı, daha az güç tüketen ASIC'ler

OMEGA ROC family (Christophe de la Taille)
Argonne-Fermilab DCAL ASIC (Gary Drake)
Boston-Fermilab QIE (Eric Hazen)

Kalorimetri

Nükleer ve parçacık fiziğinde kalorimetri, parçacıkların tespiti ve özelliklerinin ölçülmesi amacıyla, bir madde bloğunda (kalorimetre) tam soğurma yoluyla gerçekleştirilen bir süreçtir.

- Tüm kalorimetrelerin ortak özelliği, ölçüm sürecinin yıkıcı olmasıdır.
    - Örneğin, manyetik alanda parçacıkları izleyerek ölçüm yapan tel odalarından farklı olarak, kalorimetre işlemi tamamlandığında parçacıklar artık incelenmek için kullanılamaz.
    - Tek istisna müonlarla ilgilidir. Müonların önemli miktarda maddeyi geçebilmesi, müon tanısı için önemli bir yöntemdir.

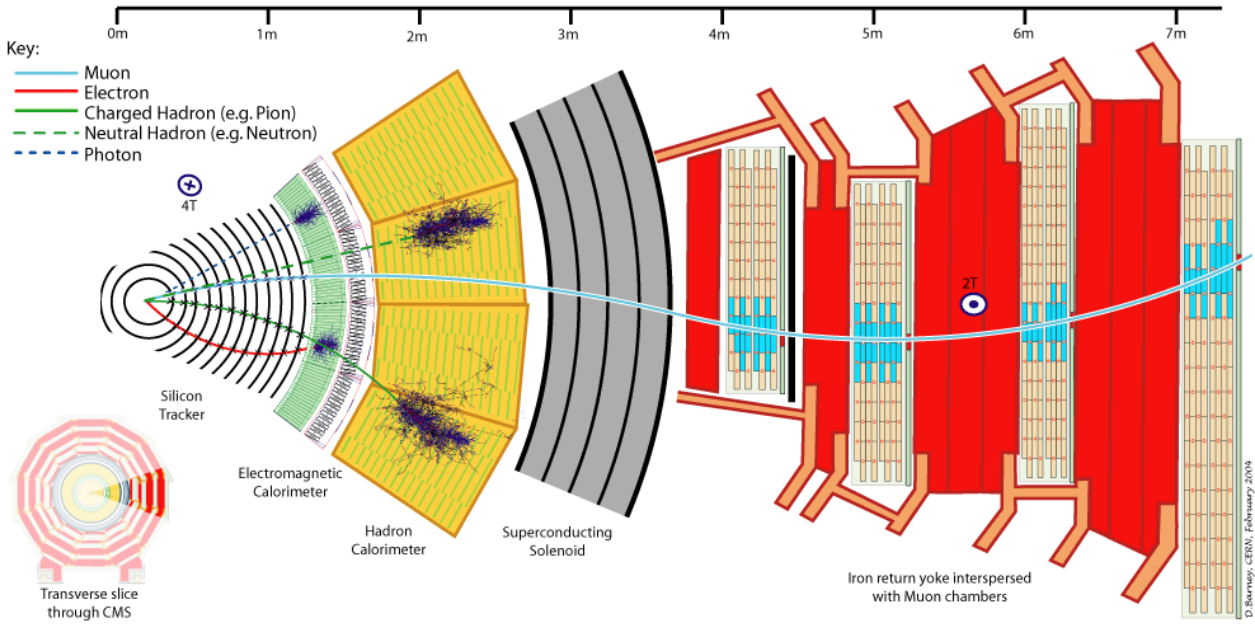

Kalorimetre Sınıfları

There are two general classes of calorimeter:

Sampling calorimeters:

Layers of passive absorber (such as Pb, or Cu) alternate with active detector layers such as Si, scintillator or liquid argon

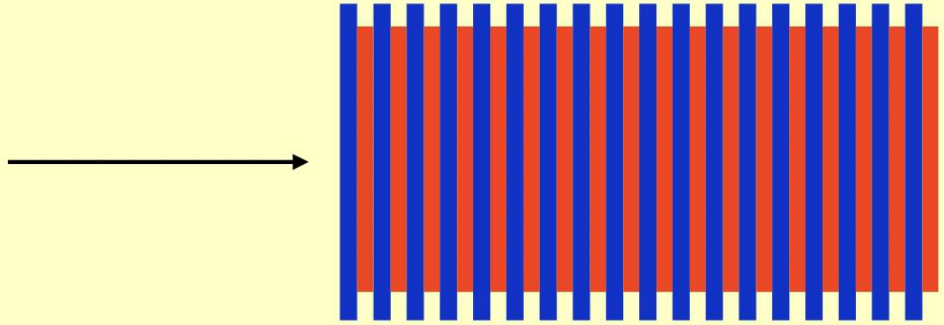

Homogeneous calorimeters:

A single medium serves as both absorber and detector, eg: liquified Xe or Kr, dense crystal scintillators (BGO, $PbWO_4$ .....), lead loaded glass.

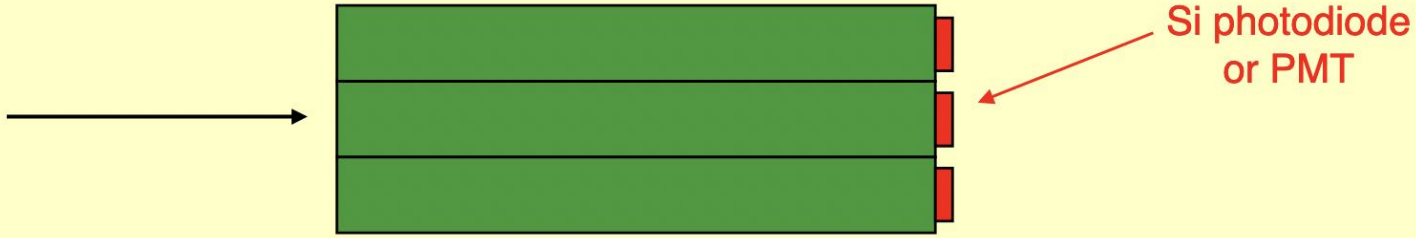

Elektromanyetik Kalorimetreler – Elektron/Pozitron/Foton

	CMS	ATLAS	ALICE	LHCb
Teknoloji	$PbWO_4$ kristal	Pb/LAr akordiyon	Pb-sintilatör shashlik	Pb-sintilatör shashlik

	ATLAS		CMS	
Intrinsic resolution	Barrel	End caps	Barrel	End caps
Stochastic term a	10%	10 to 12%	3%	5.5%
Local constant term b	0.2%	0.35%	0.5%	0.5%

$$\frac{\sigma(E)}{E} = \frac{\alpha}{\sqrt{E}} \oplus C$$

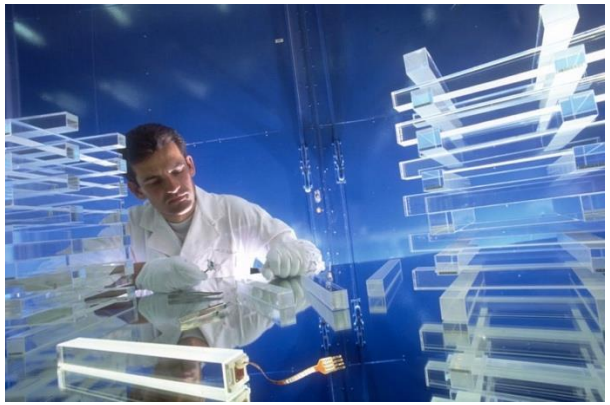

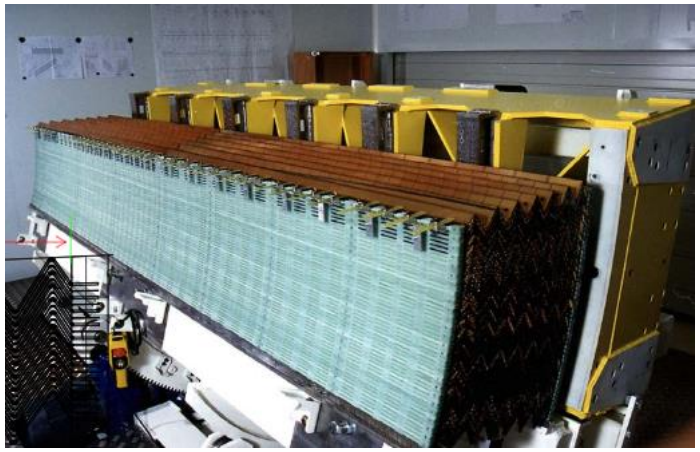

Hadron Kalorimetreleri – Hadronlar

Teknoloji	CMS	ATLAS	ALICE	LHCb
Barrel	Brass-scintillator tile	Fe-scintillator tile		Fe-scintillator tile
Forward	Brass-scintillator tile Fe-quartz fiber	Cu/LAr CuW/LAr	 W-quartz fiber	

$$\frac{\sigma(E)}{E} = \frac{\alpha}{\sqrt{E}} \oplus \frac{\beta}{E} \oplus C$$

	ATLAS				CMS	
	Barrel LAr/Tile		End-cap LAr			
	Tile	Combined	HEC	Combined	Had. barrel	Combined
Electron/hadron ratio	1.36	1.37	1.49			
Stochastic term	$45\%/\sqrt{E}$	$55\%/\sqrt{E}$	$75\%/\sqrt{E}$	$85\%/\sqrt{E}$	$100\%/\sqrt{E}$	$70\%/\sqrt{E}$
Constant term	1.3%	2.3%	5.8%	$< 1\%$		8.0%
Noise	Small	3.2 GeV		1.2 GeV	Small	1 GeV

Kalorimetride Trendler - I

The HGCAL Project

5D imaging calorimeter
- 3D spatial granularity, energy, timing information
- HGCAL covers $1.5 < \eta < 3.0$
- Two separated sections in one single detector

Active Materials
- Silicon Sensors (CE-E and CE-H)
  - ~620 m^2 Si sensors in ~27000 silicon modules
  - ~6M Si Channels (0.5 or 1cm^2 cell size)
- Plastic Scintillators with SiPM readout (CE-H)
  - 240k scintillator tiles (~370 m^2)

Passive Materials
- Lead absorber plates, copper cooling plates, and CuW baseplates
- Compact and dense object → 225 T

Power Consumption
- ~125kW per endcap

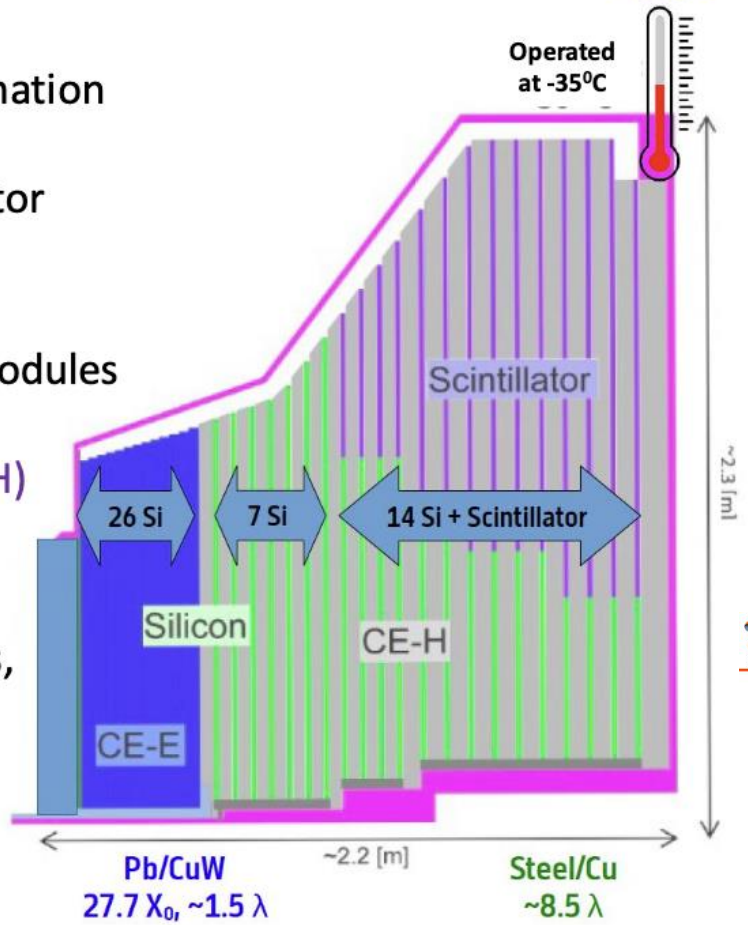

Gelecek 10+ yılın en büyük çaplı kalorimetri uygulaması.

Tüm çalışma prensibi CALICE çıktılarından esinlenmiştir.

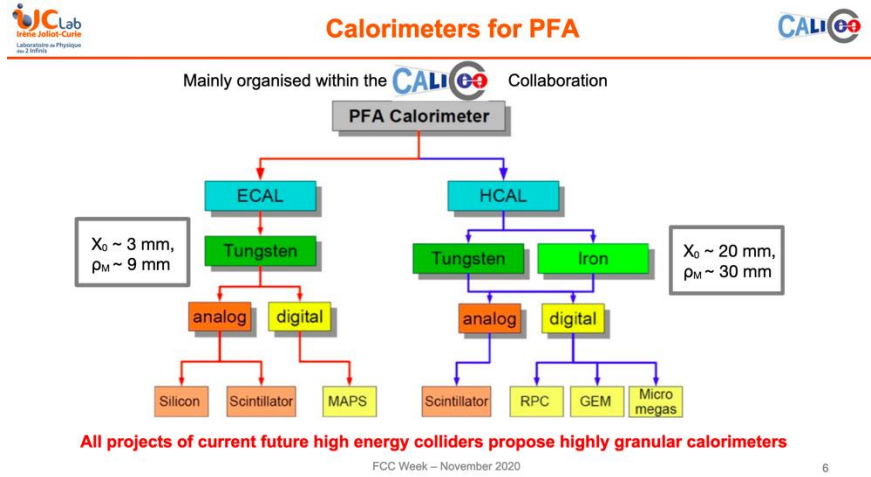

https://indico.cern.ch/event/1532019/contributions/6526245/attachments/3072502/5435923/borakagun_hgcal_yefist.pdf

Kalorimetride Trendler - II

The ADRIANO3 Triple Readout Calorimetric Technique – Burak Bilki - Corrado Gatto (evolves from dual readout calorimetry)

ADRIANO3 Active Components

- Cerenkov radiator: 3x3x2 cm^3 lead-glass tiles (typical size)
- Scintillator component: 3x3x 0.5 cm^3 scintillating tiles (typical size)
- Neutron component: 1x1x0.5 cm^3 doped RPC
- Tiles readout: on-tile sipm
- RPC readout: pads

https://indico.cern.ch/event/1368231/contributions/5894558/attachments/2834632/4953314/DRD6-CERN20240406_v3.pdf

Secondary Emission Calorimetry – Burak Bilki et al.

Construction of SE Calorimeter Modules

SE modules with 7 Hamamatsu R7761 19 stage mesh dynode PMTs were constructed. The baseboards were designed to provide three operation modes:

- Normal divider (photomultiplier) mode
- Cathode – first dynode shorted mode
- Floating cathode mode

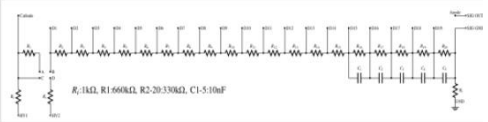

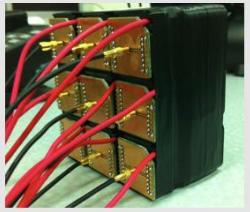

The default operation mode for the SE module was the cathode - first dynode shorted mode (B-C bridge) with an average gain of 6-9×10^5.

E. Tiras, et.al., JINST 11 P10004, 2016

https://indico.cern.ch/event/1339557/contributions/5898471/attachments/2859965/5003437/CALOR2024_SE_Bilki.pdf

The GRAiNITA Concept

The GRAiNITA concept: a new EM calorimeter for FCCe+e- experiments

Opaque scintillator technique for the development of a new Shashlik calorimeter with extremely fine sampling

Shashlik calorimeter: alternating layers of scintillator and absorber

$\sigma_E/E \sim 10\%/\sqrt{E}$ [1]

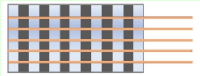

GRAiNITA: mix of scintillators grains soaked in a liquid as absorber

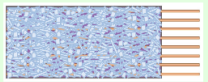

→ For improved energy resolution and very good sampling
→ For costs reduction: grains production is 2.5 less expensive than volumetric crystals
→ For good energy measurements of the jets via de scintillator via the PSD

$ZnWO_4$
- LY= 10 000 ph/MeV
- Z_{eff}=61
- Density 7.62 g/cm^3
- n=2.1-2.3
- τ = 20 μs
- λ^{em}_{max} = 490 nm
- Grown in grain size

- High-Z and high-density grains: $ZnWO_4$
- High-density and high-refractive index liquid: **LST fastfloat, $NaWO_4$ solution**
- WLS fibers to collect the scintillation light: **O2(200) coupled to SiPMs**

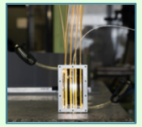

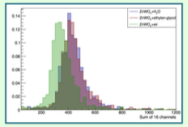

For the small-size prototype: **LY = O(400phe/40MeV) [2]**

https://ieeexplore.ieee.org/document/10656876

Geniş Hacimli Asal Sıvı Dedektörleri - Nötrinolar

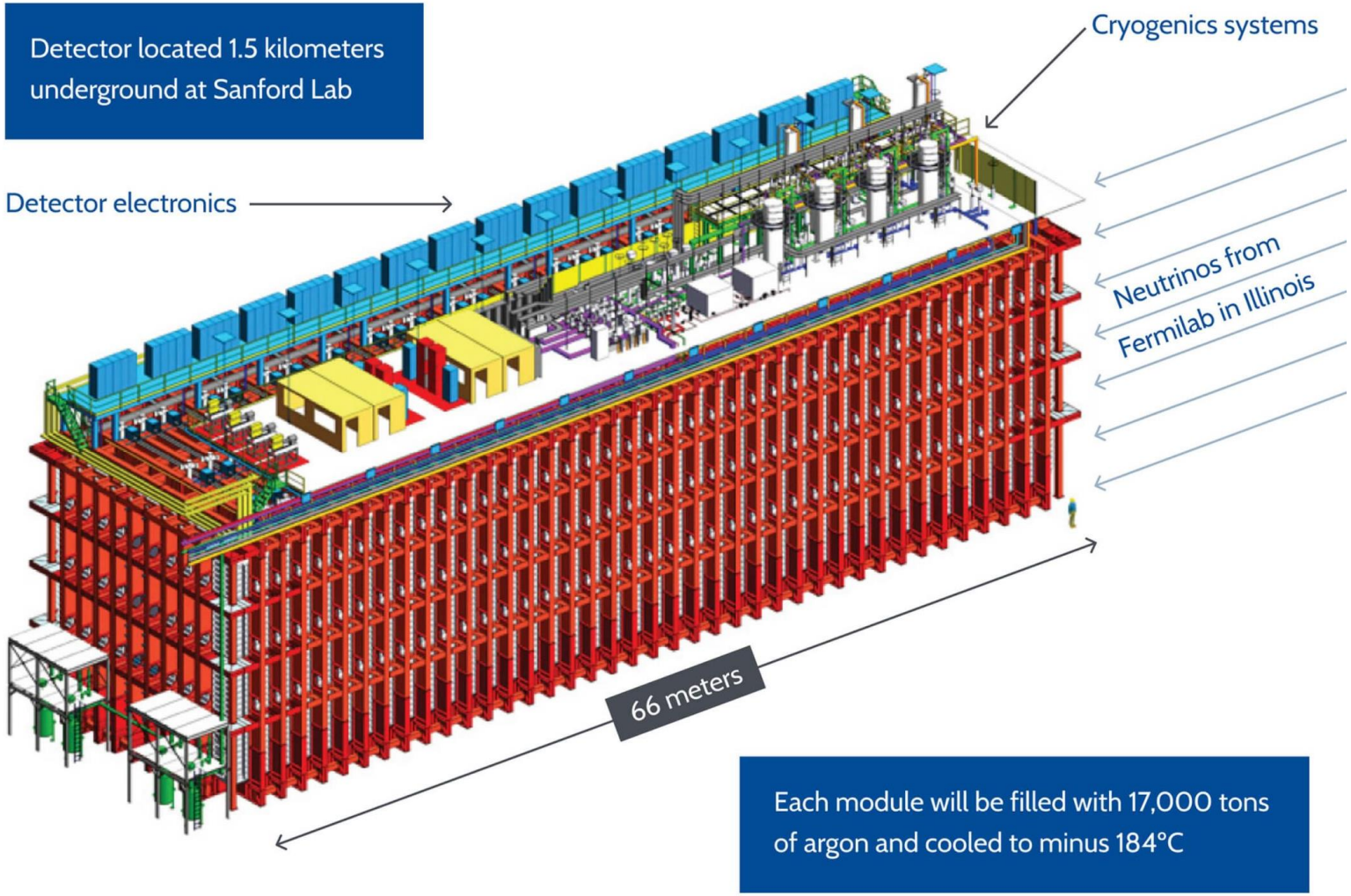

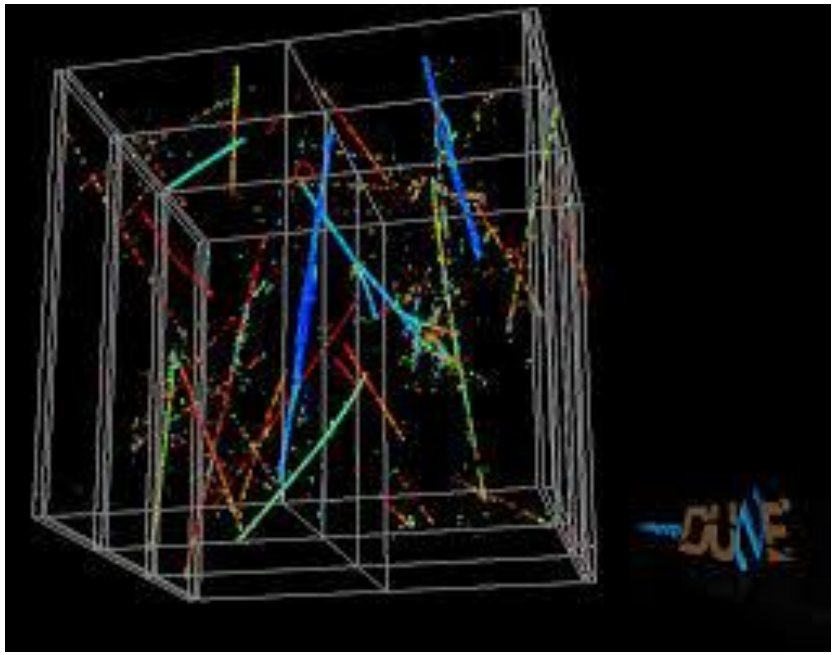

Özet

Parçacık fiziğinin 100 yılı ve bu süre zarfındaki keşifler, geniş bir yelpazedeki enstrümanlar ve teknikler sayesinde mümkün olmuştur.

- Günümüz parçacık dedektörleri, tüm olası teknikleri birleştirerek parçacıkların "elektronik görüntülerini" oluşturur.

- Yüksek segmantasyonlu görüntüleme cihazları hassasiyet açısından rakipsizdir, ancak yavaştır ve tetiklenemezler (?). Ancak bu alanın geleceğini oluşturmaktadırlar.

- Bir parçacığı tespit edebilmek için, onun etkileşime girmesi ve enerji bırakması gereklidir. Bu nedenle, mümkün olan tüm etkileşim türlerini kullanarak olası tüm elektronik sinyalleri oluşturma yönündeki tüm yöntemler denenmelidir.